



Original article

Rational design, efficient syntheses and biological evaluation of *N,N'*-symmetrically bis-substituted butylimidazole analogs as a new class of potent Angiotensin II receptor blockers

George Agelis^{a,1,*}, Amalia Resvani^{a,1}, Catherine Koukoulitsa^b, Tereza Tůmová^c, Jiřina Slaninová^c, Dimitra Kalavrizioti^d, Katerina Spyridaki^e, Antreas Afantitis^f, Georgia Melagraki^f, Athanasia Sifaka^g, Eleni Gkini^g, Grigorios Megariotis^h, Simona Golic Grdadolnik^{i,j}, Manthos G. Papadopoulos^h, Demetrios Vlahakos^k, Michael Maragoudakis^d, George Liapakis^e, Thomas Mavromoustakos^b, John Matsoukas^{a,1,*}

^a Department of Chemistry, University of Patras, 26500 Patras, Greece

^b Laboratory of Organic Chemistry, Department of Chemistry, University of Athens, Panepistimiopolis-Zografou 15771, Athens, Greece

^c Institute of Organic Chemistry and Biochemistry, Academy of Sciences of the Czech Republic, Flemingovo nám. 2, 16610 Prague 6, Czech Republic

^d Department of Pharmacology, School of Medicine, University of Patras, Patras 26500, Greece

^e Department of Pharmacology, Faculty of Medicine, University of Crete, Voutes, 71003 Heraklion, Crete, Greece

^f Department of Chemoinformatics, NovaMechanics Ltd, John Kennedy, Ave 62-64 Pallouriotissa, Nicosia 1046, Cyprus

^g Laboratory of Biochemistry, Department of Chemistry, University of Athens, Zografou, 15784 Athens, Greece

^h National Hellenic Research Foundation, Institute of Organic and Pharmaceutical Chemistry, Vas. Constantinou 48, 11635 Athens, Greece

ⁱ Laboratory of Biomolecular Structure, National Institute of Chemistry, Hajdrihova 19, SI-1001 Ljubljana, Slovenia

^j EN-FIST Centre of Excellence, Dunajska 156, SI-1000 Ljubljana, Slovenia

^k Department of Internal Medicine, 'ATTIKON' University Hospital, Athens, Greece

¹ Eldrug SA, Patras Science Park, 26504 Patras, Greece

ARTICLE INFO

Article history:

Received 27 September 2012

Received in revised form

25 December 2012

Accepted 26 December 2012

Available online 2 January 2013

Keywords:

AT1 receptor blockers

N,N'-Bis-alkylated butylimidazole analogs

Synthesis

Wittig reaction

Hydroxymethylation

Structure elucidation

Docking studies

Molecular dynamics

Biological evaluation

ABSTRACT

A series of symmetrically bis-substituted imidazole analogs bearing at the N-1 and N-3 two biphenyl moieties ortho substituted either with tetrazole or carboxylate functional groups was designed based on docking studies and utilizing for the first time an extra hydrophobic binding cleft of AT1 receptor. The synthesized analogs were evaluated for their *in vitro* antagonistic activities (pA_2 values) and binding affinities ($-\log IC_{50}$ values) to the Angiotensin II AT1 receptor. Among them, the potassium ($-\log IC_{50} = 9.04$) and the sodium ($-\log IC_{50} = 8.54$) salts of 4-butyl-*N,N'*-bis[2'-(2*H*-tetrazol-5-yl)biphenyl-4-yl]methyl]imidazolium bromide (**12a** and **12b**, respectively) as well as its free acid **11** ($-\log IC_{50} = 9.46$) and the 4-butyl-2-hydroxymethyl-*N,N'*-bis[2'-(2*H*-tetrazol-5-yl)biphenyl-4-yl]methyl]imidazolium bromide (**14**) ($-\log IC_{50} = 8.37$, $pA_2 = 8.58$) showed high binding affinity to the AT1 receptor and high antagonistic activity (potency). The potency was similar or even superior to that of Losartan ($-\log IC_{50} = 8.25$, $pA_2 = 8.25$). On the contrary, 2-butyl-*N,N'*-bis[2'-(2*H*-tetrazol-5-yl)biphenyl-4-yl]methyl]imidazolium bromide (**27**) ($-\log IC_{50} = 5.77$) and 2-butyl-4-chloro-5-hydroxymethyl-*N,N'*-bis[2'-(2*H*-tetrazol-5-yl)biphenyl-4-yl]methyl]imidazolium bromide (**30**) ($-\log IC_{50} = 6.38$) displayed very low binding affinity indicating that the orientation of the *n*-butyl group is of primary importance. Docking studies of the representative highly active **12b** clearly showed that this molecule has an extra hydrophobic binding feature compared to prototype drug Losartan and it fits to the extra hydrophobic cavity. These results may contribute to the discovery and development of a new class of biologically active molecules through bis-alkylation of the imidazole ring by a convenient and cost effective synthetic strategy.

© 2013 Elsevier Masson SAS. All rights reserved.

* Corresponding authors. Department of Chemistry, University of Patras, 26500 Patras, Greece. Tel.: +30 6944514458.

E-mail addresses: aggelisgeorge@hotmail.com (G. Agelis), imats@upatras.gr (J. Matsoukas).

¹ The first two authors contributed equally to this work.

1. Introduction

The Renin–Angiotensin System (RAS) plays a key role in regulating cardiovascular homeostasis and electrolyte/fluid balance in normotensive and hypertensive subjects. In the RAS the biological

actions of Angiotensin II (ANGII), such as vasoconstriction, release of aldosterone, stimulation of sympathetic transmission and cellular growth are mediated by the Angiotensin type 1 (AT1) receptor. Consequently, the RAS has been the prime target for the therapy of cardiovascular diseases and non-peptide AT1 receptor antagonists have been developed to specifically block it [1,2]. In specific, the DuPont group pursued a study in this field and developed Losartan, the first orally effective non-peptide antagonist, which is *in vivo* metabolized to the more potent EXP 3174 [3] (Fig. 1). Since then, numerous new antagonists have been reported by various research groups with nine of them in the clinic i.e. Candesartan [4], Valsartan [5], Irbesartan [6], Telmisartan [7], Olmesartan [8] which have been established as strong AT1 Receptor Blockers (ARBs). On 25 February 2011, the U.S. Food and Drug Administration (FDA) approved Azilsartan medoxomil [9,10] which is a newer-generation ARB, for the treatment of high blood pressure in adults. Despite the plethora of treatment options for the management of hypertension, 56% of patients do not have their blood pressure under adequate control [11] suggesting the need for the development of improved ARBs.

The majority of selective ARBs have resulted from the strategy of modifying or replacing several pharmacophore groups of Losartan. Structure Activity Relationship (SAR) studies of Losartan and other imidazole blockers have been reported. Lipophilic substituents, such as the biphenylmethyl group at the 1-position [12], a linear alkyl group at the 2-position [13,14] and an acidic group, like tetrazole, CO₂H, or NHSO₂CF₃ on the biphenylmethyl group [4,7,15], are required for antagonistic activity. Furthermore, the DuPont group recommended a lipophilic and electron-withdrawing group,

such as iodine or CF₃, as a substituent at the 4-position and a small-sized group at the 5-position, such as CH₂OH, CH₂OMe, or CO₂H, which is capable of forming a hydrogen bond [8,9].

We recently described a series of *N*-substituted 5-butylimidazole analogs as potent ARBs via efficient synthetic routes, allowing the facile introduction of substituents on the imidazole ring [16–19]. Based on these findings, we rationally designed a new class of *N,N'*-symmetrically bis-substituted butylimidazole analogs as potent ARBs that occupy an extra hydrophobic binding cleft (Fig. 1). Thus, in the present work, a series of new compounds has been synthesized bearing (i) an imidazole ring; (ii) the biphenylmethyl moiety at the *N*-1 and *N*-3 of the heterocyclic ring; (iii) an acidic functionality such as a tetrazole group or its bioisostere carboxy group ortho substituted at the biphenylmethyl group, and (iv) the *n*-butyl chain substituted on the heterocyclic ring at the C-2 or C-5 for efficient binding to the receptor. Furthermore, the hydroxymethyl group was introduced at the C-2 as well as a halogen atom at the C-4 of the imidazole ring, since the chloro substituent in the DuPont series interacts with a lipophilic pocket of the receptor [10].

These unusual analogs were *in vitro* evaluated by means of their binding affinities for the human AT1 receptor, as well as for their ability to inhibit the contractility effect of ANGI in isolated rat uterus, compared to Losartan. The SAR study was performed and the results suggested that the position of the *n*-butyl group in this *N,N'*-bis-alkylated series plays a significant role in the interaction with the AT1 receptor. Finally, structure elucidation and detailed docking studies have been carried out for the one of the most potent synthetic analog **12b**.

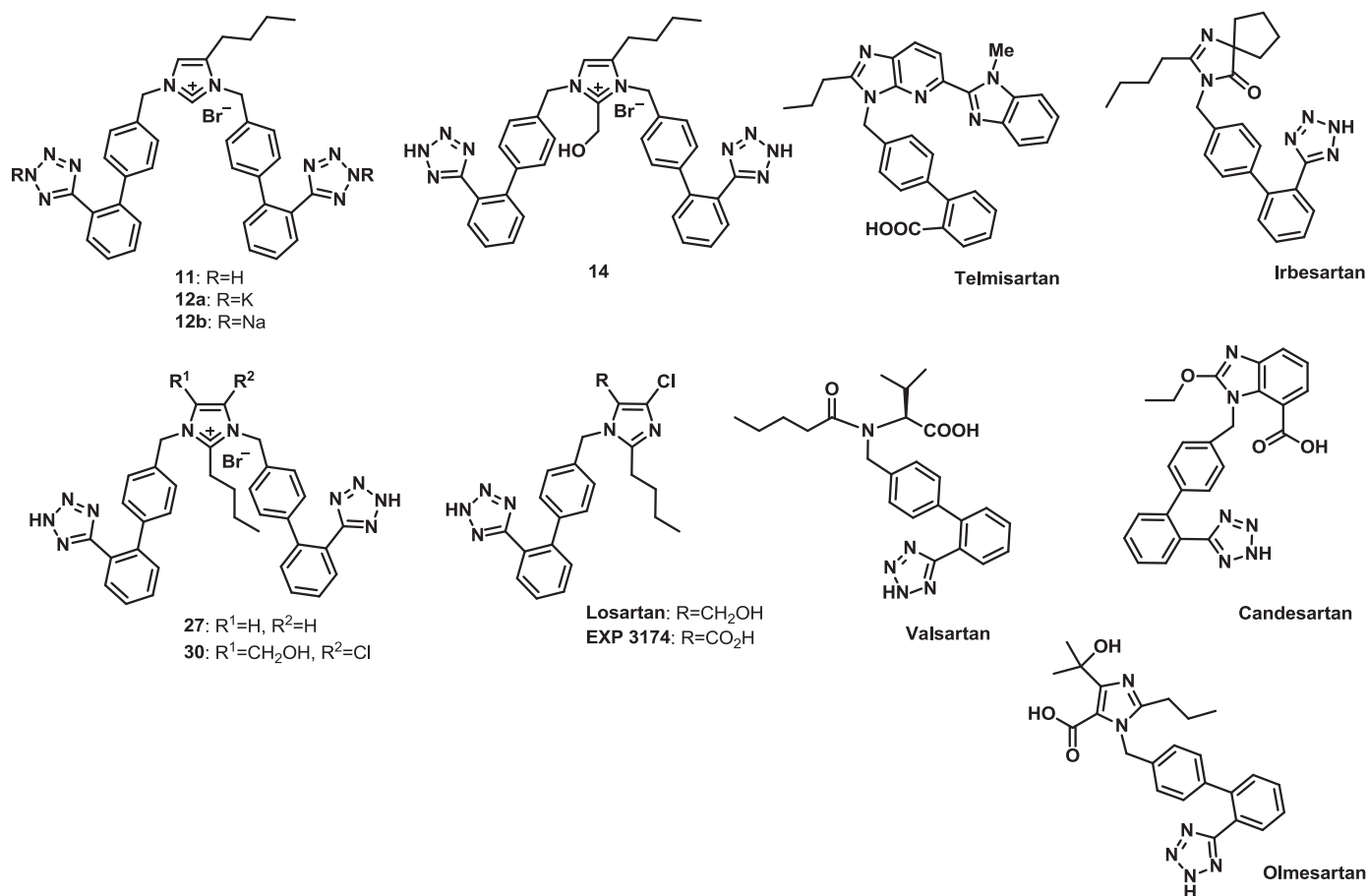


Fig. 1. Selected bis-alkylated butylimidazole synthesized analogs, Losartan, EXP 3174 (*in vivo* active metabolite) and ARBs marketed for hypertension.

2. Results and discussion

2.1. Chemistry

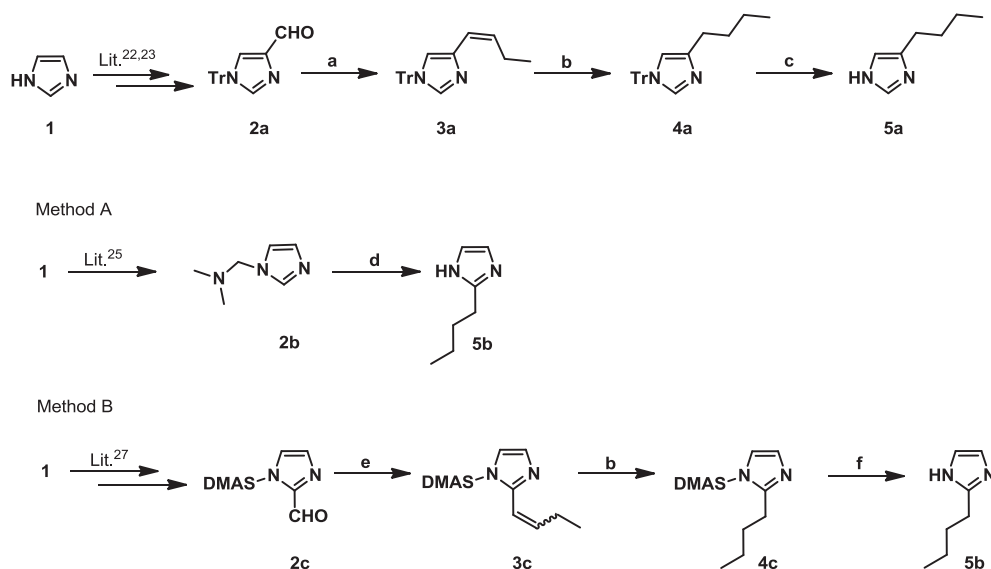
In the current study, we initially examined various synthetic protocols for the syntheses of 4(5)- and 2-substituted imidazoles as key precursors for the preparation of *N,N'*-bis-alkylated analogs as potent ARBs. In Scheme 1, the syntheses of 4(5)- and 2-butylimidazole via a synthetic sequence involving different *N*-protected imidazole groups are depicted. Imidazole (**1**) was readily transformed through a four-step synthetic pathway into the corresponding 1-trityl-imidazole-4-carboxaldehyde (**2a**) [20,21]. Wittig reaction [22] of the carboxaldehyde **2a** by treatment with NaH and the nonstabilized *n*-propyl triphenylphosphonium bromide ($\text{CH}_3\text{CH}_2\text{CH}_2\text{PPh}_3\text{Br}$) in THF at rt furnished exclusively the *Z*-**3** isomer **3a** in excellent yield (81%). The *Z*-configuration was confirmed by ^1H NMR which showed the presence of two vinylic protons at 6.25 and 5.60 ppm as doublet of triplets, respectively ($J = 11.6$ Hz). The latter was subjected to catalytic hydrogenation under H_2 atmosphere (3 bar) in the presence of Pd/C at ambient temperature for 2 h to give **4a** in 92% yield. Finally, demasking of NH by treatment with 20% TFA in CH_2Cl_2 in the presence of Et_3SiH as scavenger furnished the target 4(5)-butylimidazole (**5a**).

Two routes were investigated for the conversion of **1** into the 2-butylimidazole (**5b**). In the first approach (Scheme 1, Method A), the *N*-1 was protected with the (*N*-dimethylamino)methyl group under Mannich reaction conditions [23] resulting in **2b**. Then, the latter compound underwent smooth lithiation, which occurred regioselectively at the 2-position of the imidazole ring, upon treatment with 1.6 M *n*-BuLi in the presence of 1,3-dimethyl-3,4,5,6-tetrahydro-2(1*H*)-pyrimidinone (DMPU) in THF at -78 °C, followed by electrophilic quenching with *n*-BuI [23,24]. Subsequent facile acidic hydrolysis of the protective group afforded the corresponding 2-butylimidazole (**5b**) in 85% yield. In the second approach (Scheme 1, Method B), carboxaldehyde **2c** was prepared as described in the published procedure [25] using the *N,N*-dimethylsulfamoyl group (DMAS) as NH protective group for the lithiation/electrophilic quenching sequence. Wittig reaction of **2c** by treatment with NaH and $\text{CH}_3\text{CH}_2\text{CH}_2\text{PPh}_3\text{Br}$ in the presence of *t*-amyl alcohol [26,27] in THF at 0 °C to rt proceeded smoothly leading to the anticipated olefin **3c** as a mixture of *Z* and *E* isomers in a ratio of ca. 3:1 (as indicated by

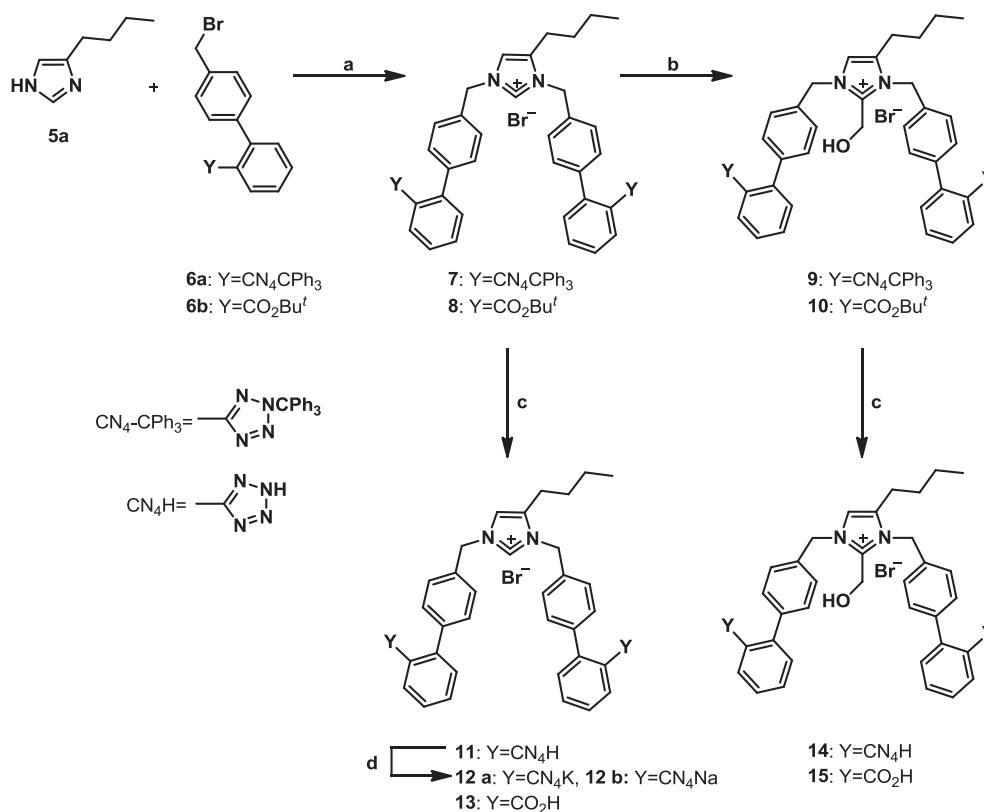
HPLC) which were isolated and identified by NMR in 62% and 24% yield, respectively. Then, the isomers were subjected to catalytic hydrogenation to afford the saturated **4c** in excellent yield (90%). Finally, hydrolysis of **4c** in refluxing 1.5 N HCl [28] afforded the target compound 2-butylimidazole (**5b**). The two methods are quite similar with respect to yields and final products, however, the former was proven to be more efficient in terms of total steps.

In Scheme 2, the syntheses of *N,N'*-bis-alkylated butylimidazole derivatives bearing the biphenylmethyl moiety ortho substituted either with the tetrazole or its bioisostere carboxy group as well as the hydroxymethyl group at the 2-position are depicted. The *N,N'*-bis-alkylation was generally accomplished under basic conditions [29] followed by the treatment of the resulting salt with the appropriate alkylating agent in excess. 4(5)-Butylimidazole (**5a**) was converted to the corresponding quaternary salts **7** and **8** under the general heterogeneous phase alkylation protocol. In particular, the latter compounds were obtained using excess of the biphenylmethyl bromides **6a** and **6b** [19] (2.3 equiv.) in the presence of K_2CO_3 in anhydrous DMF at ambient temperature for 8 h in 78–82% yields. Then, hydroxymethylation was promptly carried out in a sealed tube by treatment with diisopropylethylamine and 37% formalin in DMF at 85 °C for 1 h [17,19]. This reaction proceeded quantitatively as indicated by HPLC and led rapidly and exclusively to the desired hydroxymethylated products **9** and **10**. The trityl and *t*-Bu groups of **7**, **9** and **8**, **10**, respectively, were promptly removed upon addition of 20% trifluoroacetic acid (TFA) in CH_2Cl_2 in the presence of Et_3SiH as scavenger to obtain the final compounds **11**, **13**, **14**, **15** in 72–85% yields. Finally, conversion of **11** into the corresponding water soluble bis-potassium and sodium salts **12a** and **12b** was accomplished by treatment with KOH and NaOH, respectively, in $\text{MeOH-H}_2\text{O}$ at rt for 5 h in 80–83% yields. The ^1H NMR spectrum of **12a** showed two methylene signals of *N*-1 and *N*-3 at 5.33 and 5.32 ppm as singlet peaks, the H-5 of imidazole at 7.41 ppm and H-2 at 8.93 ppm also as singlet peaks. In addition, the hydroxymethylated analog of **14** showed the absence of the proton at C-2 and the appearance of a singlet peak at 4.92 ppm, corresponding to the hydroxymethylene protons.

In Scheme 3, the syntheses of *N,N'*-bis-alkylated halogenated butylimidazole derivatives bearing the biphenylmethyl moiety ortho substituted either with the tetrazole or its bioisostere carboxy group



Scheme 1. Reagents and conditions: (a) $\text{CH}_3\text{CH}_2\text{CH}_2\text{PPh}_3\text{Br}$, NaH (powdered, 95%), THF, rt, 8 h; (b) H_2 (3 bar), 10% Pd/C, MeOH, rt, 2 h; (c) 20% TFA in CH_2Cl_2 , Et_3SiH , rt, 1 h; (d) *n*-BuLi (1.6 M in hexanes), DMPU, *n*-BuI, then 2 M HCl; (e) $\text{CH}_3\text{CH}_2\text{CH}_2\text{PPh}_3\text{Br}$, NaH (powdered, 95%), *t*-amyl alcohol, THF, 0 °C to rt, 10 h; (f) 1.5 N HCl, THF, reflux, 2 h.



Scheme 2. Reagents and conditions: (a) K₂CO₃, DMF, rt, 8 h; (b) 37% formalin, diisopropylethylamine, DMF, 80 °C, 1 h; (c) 30% TFA in CH₂Cl₂, Et₃SiH, rt, 1 h; (d) KOH, MeOH–H₂O, rt, 5 h for **12a**, NaOH, MeOH–H₂O, rt, 5 h for **12b**.

as well as the hydroxymethyl group at the 2-position are depicted. The *N,N'*-bis-alkylation was advantageously accomplished under basic conditions by solid–liquid phase transfer catalysis (PTC) [30,31]. 4(5)-Butylimidazole (**5a**) was converted to the corresponding halogenated analogs **16c–e** by treatment with NXS (X = Cl, Br, I) in DMF in 71–73% yields. The ¹H NMR spectra of **16c–e** showed the absence of the H-4 signal of the imidazole ring at 6.74 ppm. Furthermore, the ¹³C NMR spectra showed an upfield trend in C-4 chemical shifts produced by bromine and iodine atoms for **16d** and **16e**, at 114.53 and 81.92 ppm, respectively, while the C-4 in the chloro derivative **16c** appeared at 124.24 ppm. Alkylation of **16c–e** with the alkylating agent **6a**, in the presence of K₂CO₃ and catalytic amount 18-crown-6-ether to assist by chelating potassium in anhydrous THF under reflux for 12 h, furnished the **17c–e** in 52–57% yields. PTC was also successfully adopted for the syntheses of **18c–e** by treatment with **6b** in the presence of fine powdered KOH and catalytic amount of 18-crown-6-ether in anhydrous Tol at 80 °C for 12 h in 58–64% yields. Acidolysis of protective groups in **17c–e** and **18c–e** was accomplished in the same manner and afforded **19c–e** and **20c–e**, respectively, in 73–82% yields. On the other hand, hydroxymethylation of **17c–e** and **18c–e** by treatment with 37% formalin in the presence of diisopropylethylamine in DMF at 80 °C for 1 h afforded **21c–e** and **22c–e** in 70–78% yields. The latter were subjected to acid hydrolysis with TFA, resulting in **23c–e** and **24c–e** in 75–81% yields.

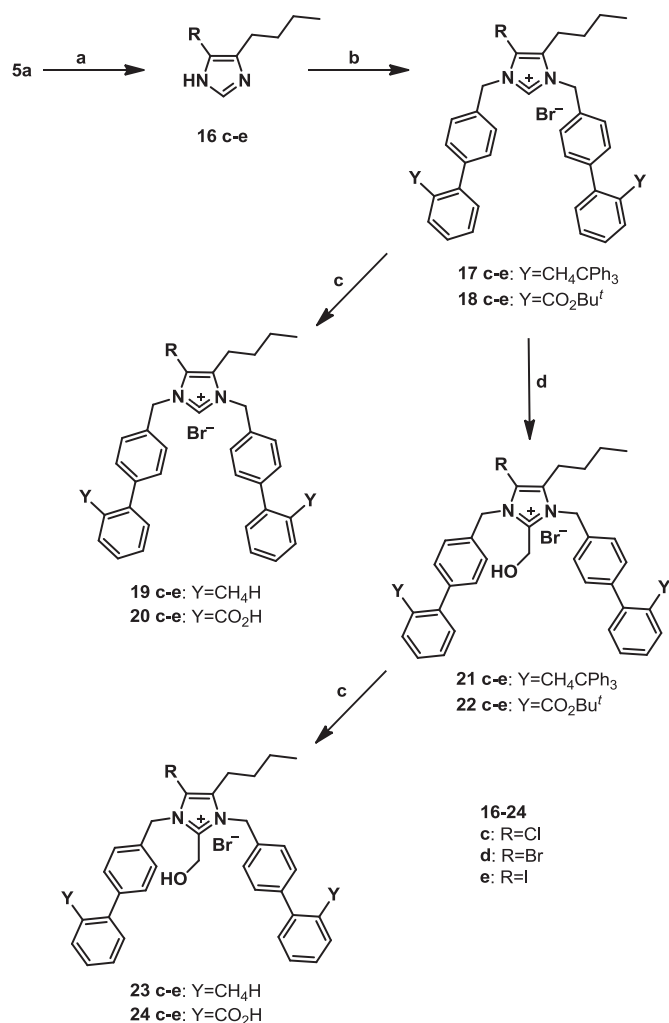
Identical methodology was employed for the preparation of 2-butylimidazole analogs **27** and **28** (Scheme 4) through a two-step sequence. In particular, alkylation of **5b** by treatment with the alkylating agents **6a** and **6b** and subsequent acid hydrolysis afforded the expected analogs **27** and **28**.

Finally, in Scheme 5, the syntheses of bis-alkylated analogs **30** and **31** with the implementation of a facile PTC alkylation–

deprotection reaction sequence in one-pot procedure are depicted. Thus, alkylation under basic conditions of the commercially available (2-*n*-butyl-4-chloro-1*H*-imidazole-4-yl)methanol **29**, which is an important precursor for the preparation of Losartan, followed by acid hydrolysis, afforded the corresponding analogs **30** and **32** in 77% and 74% yield over two steps, respectively.

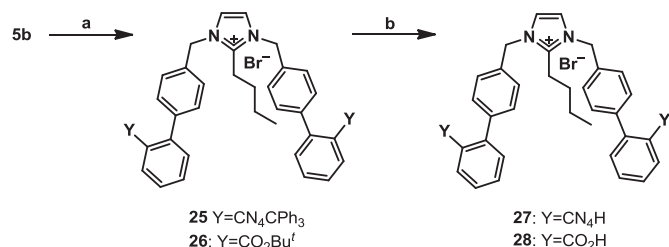
2.2. Structure elucidation of analog **12b**

The chemical structure of **12b** (Fig. 2) has been elucidated using a combination of 2D DQF-COSY and 2D ROESY experiments (Table 1). The alkyl chain of the molecule was easily identified from the 2D DQF-COSY experiment, the multiplicity and integration of the peaks (Fig. 2). Due to the asymmetry of the molecule the aromatic biphenyl protons showed distinct resonances confirmed by the integration of the peaks (see the alkyl chain extended only to one side of biphenyltetrazole moiety). The H10 and H10' protons are magnetically un-equivalent and are depicted as separate single peaks (Fig. 2). 2D DQF-COSY (Supporting information SF1) made possible to assign all aromatic peaks in combination with 2D ROESY experiment. H10 showed ROE with the single peak at 6.85 ppm, which according to the integration corresponds to the resonance of four protons. These were assigned as the H12, H13, H15, H16 protons of the aromatic ring A (Supporting information SF2). 2D ROESY spectrum reveals that this peak is correlated with the protons of the alkyl chain H6, H7, and H8 (Supporting information SF3). Similarly H10' showed ROE with the doublet at 7.04 ppm attributed to the protons 13', 15' and 18' (Supporting information SF2). The 2D DQF-COSY experiment confirmed the proposed assignment (Supporting information SF2). The doublet resonating at 6.86 ppm and assigned to 12' and 16' protons is correlated through coupling with the

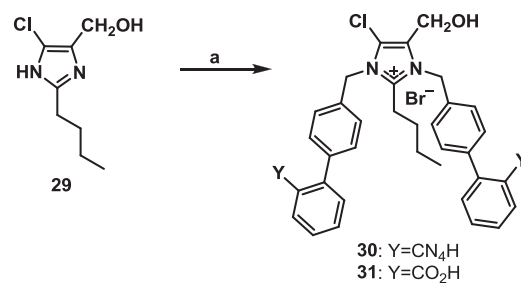


Scheme 3. Reagents and conditions: (a) NXS (X = Cl, Br, I), DMF 0 °C → rt; (b) **16c-e** → **17c-e**: **6a**, K₂CO₃, 18-crown-6, THF, reflux, 12 h and **16c-e** → **18c-e**: **6b**, KOH, 18-crown-6, Tol, 80 °C, 12 h; (c) 30% TFA in CH₂Cl₂, Et₃SiH, rt, 1 h; (d) 37% formalin, diisopropylethylamine, DMF, 80 °C, 1 h.

doublet at 7.04 ppm. Such correlation is evident also with Losartan molecule that contains biphenyltetrazole segment [32]. As the integration of the doublet shows the existence of three protons, the other one is assigned to H18'. This is because H18' shows correlation with the triplet peak resonating at 7.25 ppm and assigned to H19'. Consequently, H19' is correlated with multiplet at 7.31 ppm, assigned to H20', which in turn is correlating with the doublet peak at 7.55 ppm assigned to H21'. The doublet at 7.55 ppm is integrated to two protons assigned to 21, 21'. This is in accordance with results obtained with Losartan [30]. In addition, these protons are



Scheme 4. Reagents and conditions: (a) **5b** → **25**: **6a**, K₂CO₃, DMF, rt, 8 h and **5b** → **26**: **6b**, KOH, 18-crown-6, Tol, 80 °C, 12 h; (b) 30% TFA in CH₂Cl₂, Et₃SiH, rt, 1 h.



Scheme 5. Reagents and conditions: (a) **29** → **30**: **6a**, K₂CO₃, 18-crown-6, THF, reflux, 12 h then 30% TFA in CH₂Cl₂, Et₃SiH, rt, 1 h; **29** → **31**: **6b**, KOH, 18-crown-6, Tol, 80 °C, 12 h then 30% TFA in CH₂Cl₂, Et₃SiH, rt, 1 h.

expected to be the most magnetically deshielded ones, because they are close to the tetrazole ring. Apparently, the protons of the two B and B' rings have identical or close chemical shifts since they are far away from the butyl chain that differentiates mainly the environment of aromatic protons of the A and A' rings.

The broad singlet at 6.99 ppm has no coupling through bond correlation. 2D ROESY experiment shows that this peak is correlated through space with H10' and with the protons of the alkyl chain H6, H7, and H8 (Supporting information SF2 and SF3). This peak is attributed to H5 of imidazole ring. The two different patterns of biphenyl rings are observed in our previous studies using commercial and synthetic ARBs. In Losartan [32], Valsartan [33] and Eprosartan [34] the A ring shows clearly the doublet of doublet pattern common for 1,4 bis-substituted aromatic compounds. However, in the synthetic analog V8 a singlet peak is observed that is attributed to the same ring [17,35]. It is obvious that the equivalency of the protons depends on the environment that surrounds biphenyltetrazole ring. A small peak at 8.47 ppm as a remaining peak is assigned to H2. It is the most downfield peak, which can be explained with the position of H2 between two nitrogens.

2.3. Docking studies of analog **12b** at the binding site of AT1

The synthesis of **12b** and its derivatives has been based on docking studies. The docking studies of **12b** at AT1 and its interactions with the amino acids of the active site are of particular interest. Fig. 3 illustrates the best binding pose of **12b** at the binding site of AT1 ($\Delta G = -16.21$ kcal/mol) with the hydrophilic and hydrophobic areas around the molecule. The two biphenyl moieties point to the widely extended hydrophobic area, whereas the hydrophilic area mainly surrounds the imidazole ring and is less extend around the tetrazole.

Docking calculations using the same program and protocol have pointed out the best binding pose of Losartan at the active site [17]. In comparison to **12b**, Losartan is anchored to the binding site with a lower binding affinity ($\Delta G = -12.30$ kcal/mol) reflecting its lower potency.

In Fig. 4, the superimposition of the best binding poses of **12b** and Losartan is depicted. Both ligands show similar orientation at the binding site of AT1 except the biphenyl moiety tetrazole (see A', B' rings) of **12b** which has no equivalent groups. Interestingly, this additional lipophilic part resides in a lipophilic cavity surrounded by the amino acids Leu112, Ala181, Phe182, Ile288, Ala291. These hydrophobic interactions are responsible for the enhanced binding affinity of **12b** in comparison to Losartan. It is this ability of **12b** to reside in an extra cavity that triggered our interest for synthesizing new drugs having a variety of activity. This drug molecule has resulted after trying manually various derivative compounds which could fit the extra cavity. **12b** has been suggested by the synthetic group as the drug lead bearing the technognosy of the synthetic

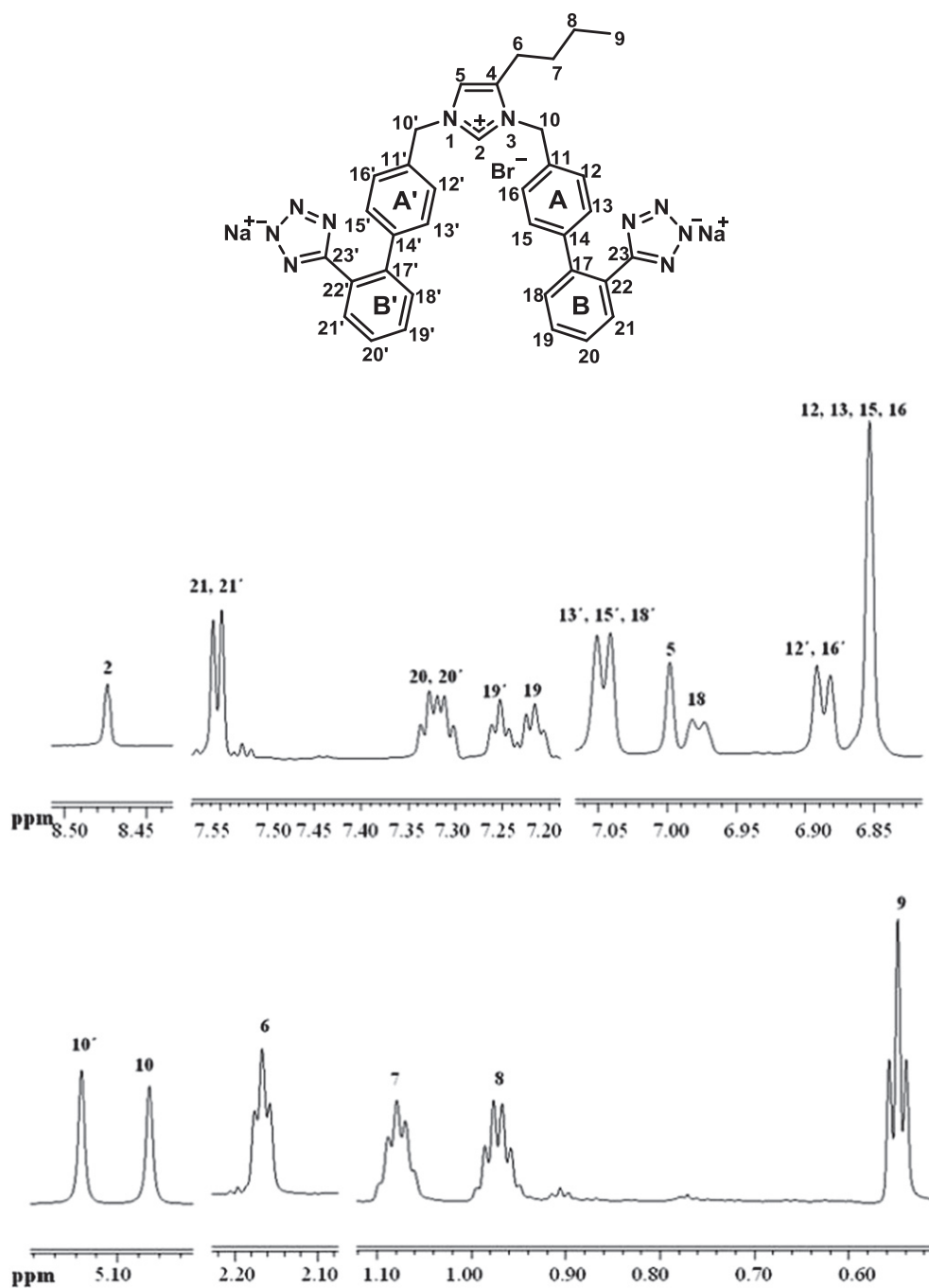


Fig. 2. ^1H NMR spectrum of analog **12b** in D_2O solvent divided into six regions for better representation, recorded on a Varian INOVA 800 MHz spectrometer at a temperature of 25°C .

feasibility of such molecules. The syntheses of this molecule and its derivatives shows that collaboration of the medicinal chemists and computational chemists can lead to new ideas and to the rational design of new classes of molecules with optimized biological activity, taking into account pharmacophore orientation and charges.

2.4. Molecular dynamics (MD) of **12b** at the binding site of AT1

It has been postulated that the molecular basis of AT1 anti-hypertensive action can be interpreted by a two-step model. In the first step, the ARB is incorporated into the membrane bilayer through the lipid–water interface and secondly laterally diffuses to reach the binding site of the AT1 receptor in order to exert its

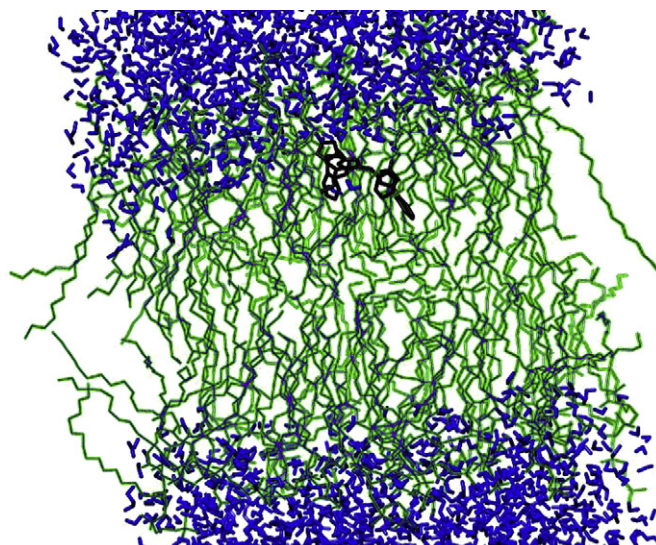
biological activity [36–38]. For this reason, we have studied not only the interaction of **12b** at the binding site of AT1 receptor but also its incorporation into plasma membrane.

Before starting the analysis of our results obtained by the MD simulation, a graphical representation of the simulated system is provided in Fig. 5(a) where **12b** (black color) included in the interior of the bilayer (dipalmitoyl phosphatidylcholine (DPPC): green color). Fig. 5(b) and (c) depicts the most preferable conformations of **12b** in decreasing order as obtained from a clustering algorithm available, which is available in the UCSF Chimera software [39]. As already mentioned, **12b** was initially placed into the water phase and during the course of the simulation penetrated into the interior of the bilayer. The mass density profiles of all components along the

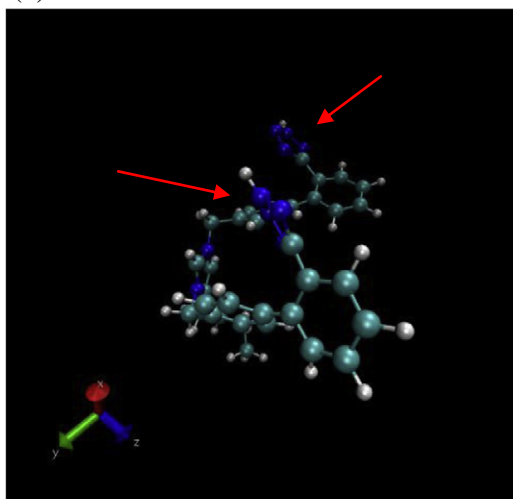
Table 1
¹H NMR (800 MHz) chemical shift assignments of **12b** in D₂O solution at 25 °C.

Hydrogen	Chemical shift (ppm)	No. of hydrogens	Multiplicity
9	0.54	3	t
8	0.97	2	m
7	1.07	2	m
6	2.16	2	t
10	5.06	2	s
10'	5.13	2	s
12, 13, 15, 16	6.85	4	bs
12', 16'	6.86	2	d
18	6.97	1	d
5	6.99	1	s
13' and 15', 18'	7.04	3	d
19	7.21	1	t
19'	7.25	1	t
20, 20'	7.31	2	m
21, 21'	7.55	2	d
2	8.47	1	s

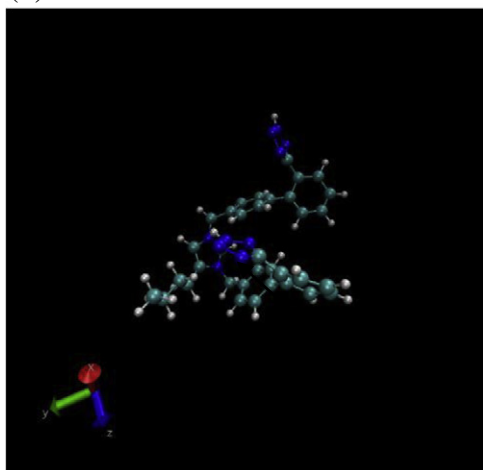
Z-axis are provided in Fig. 6; it is clearly seen that **12b** under study is found inside the bilayer (red curve). The peak of its distribution is nearly 1.1 nm far from the center of the bilayer which is defined as the minimum of the DPPC distribution (blue color). Another



(a)



(b)



(c)

Fig. 5. (a) A graphical representation of the simulated system. (b), (c) Most preferable conformations of analog **12b** in the DPPC bilayer.

interesting observation is that **12b** is found in a depth that permits an interaction with some water molecules as seen by the intercept of the distribution of water (black curve) and drug. A complementary view is given by Fig. 7, in which the distance between

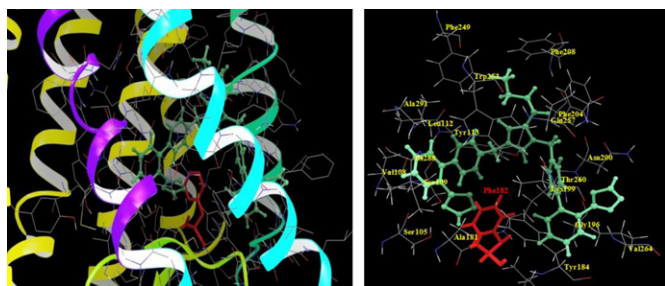


Fig. 3. Binding mode of analog **12b** at the binding site of AT1 receptor. The hydrophobic region of the binding site is shown in yellow, and the hydrophilic site that surrounds it by a 6 Å radius is shown in blue. The Phe 249 (red color) is situated between the two biphenyltetrazole moieties of analog **12b**. (For interpretation of the references to colour in this figure legend, the reader is referred to the web version of this article.)

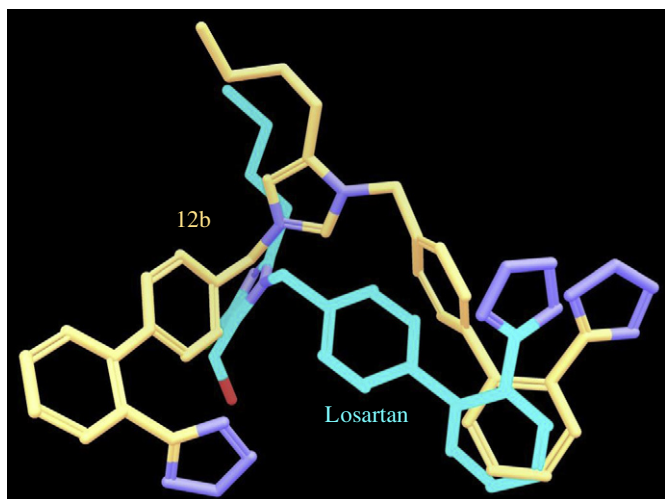


Fig. 4. Superimposition of Losartan (blue) and analog **12b** (brown). (For interpretation of the references to colour in this figure legend, the reader is referred to the web version of this article.)

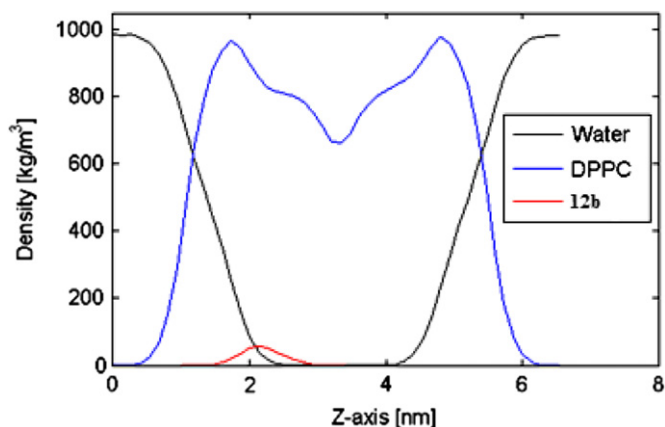


Fig. 6. Mass density profiles along the Z-axis of all components, i.e. water, DPPC and analog **12b**.

DPPC and drug centers of mass is monitored over the last 40 ns of the MD simulation. The zero in the aforementioned diagram corresponds to the center of bilayer. In order to give a clearer picture of the simulated system, the average distance of phosphorous atoms (DPPC molecules) in both leaflets is depicted as well, indicating a stable membrane with a thickness around 3.8 nm. It may also be concluded that the drug fluctuates around a distance of 1.1 nm from the bilayer center. However, it does not move significantly and therefore there is no tendency for crossing events, i.e. the move of a host molecule from one leaflet to the other through the middle of the bilayer.

The potential of mean force (PMF) of **12b** from water to lipid phase is depicted in Fig. 8, in which the zero at the abscissa corresponds to the bilayer center while remote there is pure water. The position of minimum is about 1 nm far from the bilayer center and it is compatible to the position found by the MD simulation with **12b** initially placed in the aqueous phase. Another interesting observation is the high energy barrier (41 kJ mol⁻¹) that **12b** has to overcome so as to move from one leaflet to the other through the middle of the bilayer. Besides, the free energy for partitioning into the membrane was estimated by the difference of PMF at the water phase (large distances) and at the location of the minimum. This value is approximately equal to -81 kJ mol⁻¹.

Having defined the preferred position of **12b** in the membrane from the mass density profiles and the PMF, we analyzed the

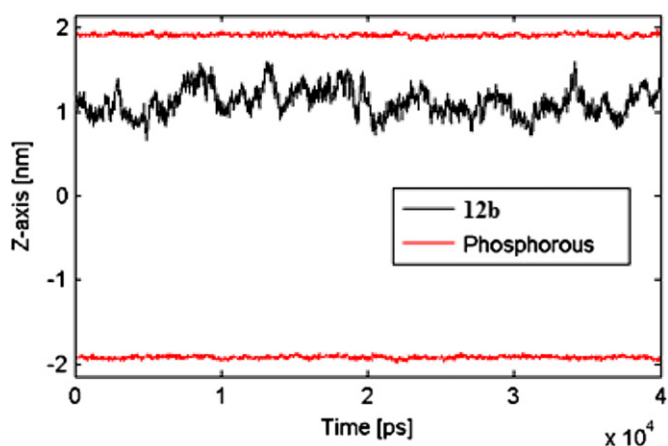


Fig. 7. Distance between analog **12b** and bilayer centers of mass. This plot is over the last 40 ns of the simulation. No crossing events were observed.

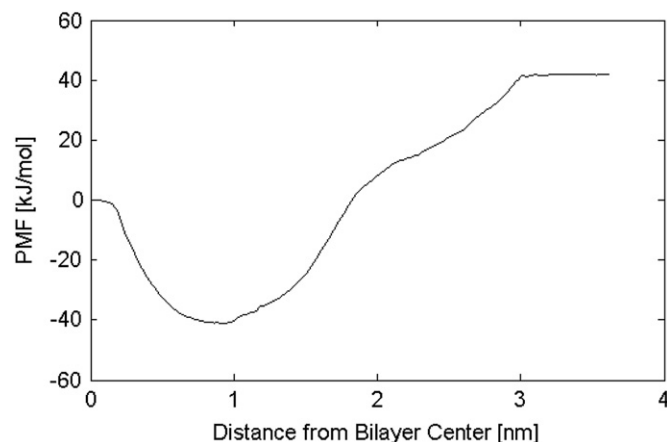


Fig. 8. PMF (along the Z-axis) of analog **12b** from water to DPPC phase.

interaction of this drug with DPPC and water molecules in terms of hydrogen bonding. To this end, a GROMACS tool was applied which makes use of standard geometrical criteria such as distance between acceptor and donor (<0.35 nm) and the angle among acceptor–hydrogen–donor (<30°). The average number of hydrogen bonds of **12b** with DPPC and the penetrated water molecules is 1.366 and 1.519, respectively, showing that indeed there is a significant interaction with these components. In particular, DPPC oxygen atoms participate in a hydrogen-bond network with two nitrogen atoms of **12b** which are indicated by two arrows in Fig. 5(b). An additional confirmation of the previous observation is provided in Fig. 9 by the fully overlapping density profiles of oxygen (DPPC) and nitrogen atoms (**12b**).

2.5. HOMO and LUMO quantum chemical calculations

Table 2 summarizes the results of HOMO and LUMO levels of the compounds studied. Based on these results, binding affinities and the *in vitro* ANGI antagonist properties, several remarks can be made. First of all, inclusion of halogens (Br, Cl, and I) in R¹ position reduced HOMO values as expected. As already mentioned HOMO energy values decrease with the presence of electron withdrawing groups (EWGs) such as halogens. A decrease in *in vitro* binding affinity as determined in radioligand binding studies for compounds **19c** and **19d** was also reported. The inclusion of a small

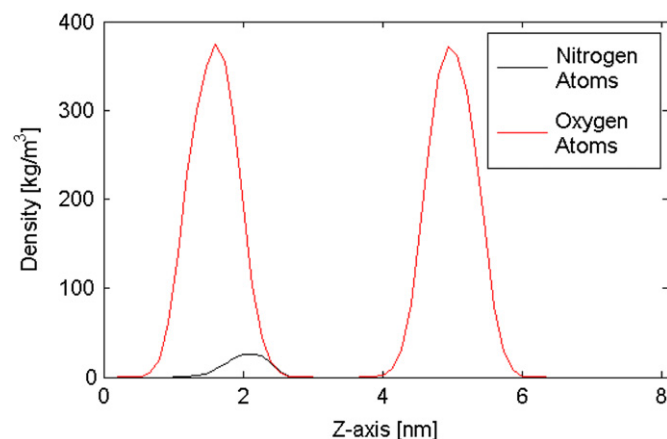


Fig. 9. Density profiles along Z-axis of DPPC oxygens and analog **12b** nitrogens. The points of black curve have been multiplied by 10 for visualization purposes.

Table 2
HOMO and LUMO energies, binding affinity expressed as $-\log IC_{50}$ values and classification of synthesized analogs according to the affinity.

Compd	HOMO (eV)	LUMO (eV)	Binding affinity $-\log IC_{50}$	Classification
11	-0.3185	-0.1449	9.46 ± 0.44	High affinity
12a	-0.26218	-0.13175	9.04 ± 0.38	High affinity
12b	-0.28058	-0.1382	8.54 ± 0.18	High affinity
14	-0.31844	-0.14207	8.37 ± 0.15	High affinity
19c	-0.30837	-0.14742	6.08 ± 0.14	Low affinity
19d	-0.30956	-0.14558	6.15 ± 0.22	Low affinity
23c	-0.31631	-0.14252	5.19 ± 0.42	Low affinity
23d	-0.31508	-0.13845	7.37 ± 0.29	High affinity
27	-0.32167	-0.13413	5.77 ± 0.46	Low affinity
30	-0.31916	-0.14134	6.38 ± 0.02	Low affinity
13	-0.33018	-0.13951	6.48 ± 0.10	Low affinity
15	-0.33136	-0.15484	6.30 ± 0.08	Low affinity

sized group such as $-CH_2OH$ (**14** and **15**) did not significantly change HOMO and LUMO values but resulted also in a reduced binding affinity. The affinity was further reduced when halogens were also included in the R^1 position (**23c**, **23d**) as expressed in *in vitro* activity (pA_2). Inclusion of K and Na (**12a** and **12b**) significantly reduced HOMO values and a decrease in binding affinity ($-\log IC_{50}$) was also reported. A switch of the substituents in R^2 and R^3 position for **11** and **27**, **19c** and **30** also resulted in a decreased activity while HOMO increased and LUMO decreased.

We have further explored the HOMO LUMO energies by developing a simple Decision Tree with the primary purpose of discriminating compounds into two categories, low affinity and high affinity, (threshold $-\log IC_{50} < 6.48$). HOMO and LUMO values were used as input variables for the development of the Decision Tree (Fig. 10) [40]. The visual inspection of the Decision Tree helps in the analysis and interpretation of the structural data, the existence of clusters and outliers, the relationship between samples and the influence of each

variable (HOMO & LUMO). The accuracy of the Decision Tree is 92%. The graphical representation of the Decision Tree for the data set is presented in Fig. 11. According to the Decision Tree, the design of new molecules as ARBs can be accomplished by high HOMO and LUMO energy values. More specifically, in the case of HOMO values are greater than -0.31916 eV and LUMO greater than -0.14252 , the compounds exert high binding affinity to the receptor. HOMO and LUMO fields are graphically depicted in Fig. 11 for **11**.

2.6. Pharmacological characterization and SAR

In order to pharmacologically characterize the synthesized analogs, we determined their binding affinities ($-\log IC_{50}$) for the human AT1 receptor in radioligand competition binding assay (Table 3, Fig. 12(a) and (b)), as well as their ability to antagonize the activity of ANGII in the rat uterus *in vitro* test (pA_2) of the high affinity compounds ($-\log IC_{50} \geq 6.50$) using Losartan as a reference compound (Table 3). Interestingly, the introduction of an additional biphenyltetrazole moiety on the 4(5)-butylimidazole led to the N,N' -bis-substituted imidazolium salt **11**, which is bound to AT1 receptor with higher affinity ($-\log IC_{50} = 9.46$) than Losartan ($-\log IC_{50} = 8.25$) (Table 3, Fig. 12). Furthermore, the water soluble potassium ($-\log IC_{50} = 9.04$) and sodium ($-\log IC_{50} = 8.54$) salts of compound **11** (**12a** and **12b**, respectively) showed slightly higher binding affinities compared to Losartan ($-\log IC_{50} = 8.25$) (Table 3, Fig. 12). Similar to binding affinities, the potency of **12b** ($pA_2 = 8.45$) to antagonize the activity of ANGII was higher compared to Losartan ($pA_2 = 8.25$). Acquisition of high binding affinity and potency has also been achieved by the introduction of the hydroxymethyl group at the C-2, resulting in **14** ($-\log IC_{50} = 8.37$, $pA_2 = 8.58$) (Table 3, Fig. 12). Replacement of the tetrazole with the bioisostere carboxy group, thus resulting in **13** and **15** significantly decreased binding affinity (Fig. 12) in line with previous studies in which tetrazole is a superior non-classical isostere of carboxylate [10,19]. More importantly, the halogenated analogs **19c**, **19d**, **23c**, **23d** (Table 3, Fig. 12) showed remarkable drop in binding affinity in contrast to the halogenated series of Losartan which retained affinity [10] indicating the ambiguous function of substituents at C-4 of imidazole [19]. Interestingly, the bis-alkylation of 2-butylimidazole and 2-butyl-4-chloro-5-hydroxymethylimidazole, the key precursor in the synthesis of Losartan, resulted in compounds **27** ($-\log IC_{50} = 5.77$) and **30** ($-\log IC_{50} = 6.38$) (Table 3, Fig. 12) displaying dramatic loss of binding affinity compared to **11**, in which the *n*-butyl group at the C-5 is exposed, thus enhancing binding to the receptor. These results suggested that the position of the *n*-butyl group plays a significant role in their interaction with the AT1 receptor.

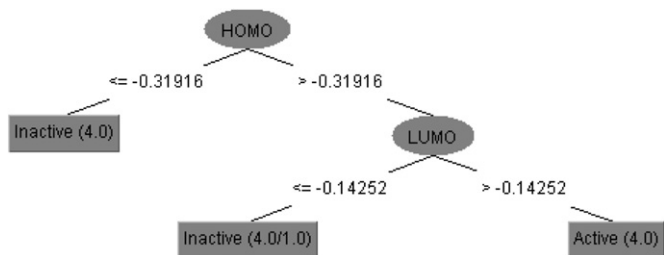


Fig. 10. Graphical representation of the Decision Tree.

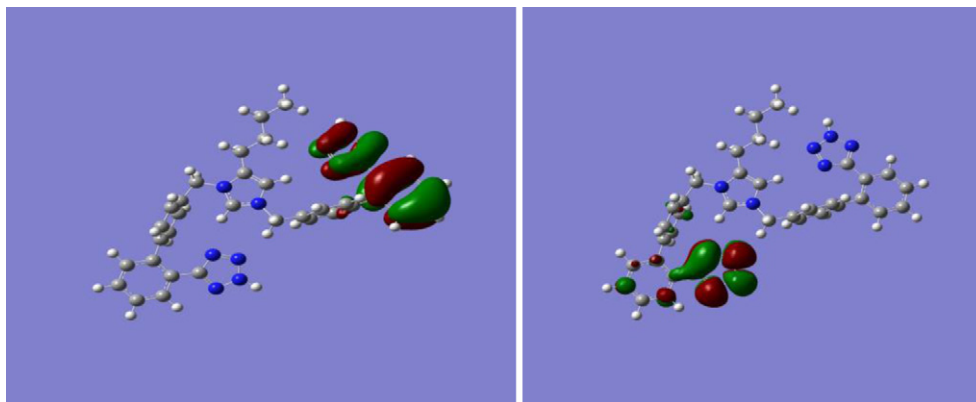
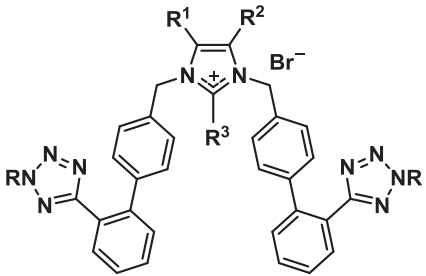
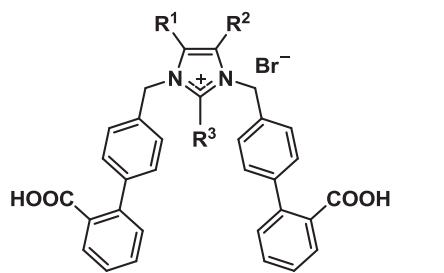


Fig. 11. HOMO and LUMO orbitals of analog **11**.

Table 3
Biological activity of synthesized analogs.



Compd	R ¹	R ²	R ³	R	Binding affinity -logIC ₅₀	Uterotonic activity <i>in vitro</i> pA ₂
11	H	Bu	H	H	9.46 ± 0.44	
12a	H	Bu	H	K	9.04 ± 0.38	
12b	H	Bu	H	Na	8.54 ± 0.18	8.45 ± 0.39
14	H	Bu	CH ₂ OH	H	8.37 ± 0.15	8.58 ± 0.39
19c	Cl	Bu	H	H	6.08 ± 0.14	
19d	Br	Bu	H	H	6.15 ± 0.22	
23c	Cl	Bu	CH ₂ OH	H	5.19 ± 0.42	
23d	Br	Bu	CH ₂ OH	H	7.37 ± 0.29	7.13 ± 0.13
27	H	H	Bu	H	5.77 ± 0.46	
30	Cl	CH ₂ OH	Bu	H	6.38 ± 0.02	
Losartan					8.25 ± 0.06	8.25 ± 0.13



13	H	Bu	H	H	6.48 ± 0.10
15	H	Bu	CH ₂ OH	H	6.30 ± 0.08

3. Conclusions

The present study refers to the design and syntheses of bis-alkylated 4(5)-butylimidazole analogs as potent ARBs. In particular, a rational design was performed to synthesize a series of *N,N'*-symmetrically bis-substituted imidazole analogs bearing at the N-1 and N-3 two biphenylmethyl moieties ortho substituted either with tetrazole or carboxylate functional groups. This work describes for the first time potent *N,N'*-bis-alkylated analogs in contrast to the marketed ARBs, which their heterocyclic core is monoalkylated. Furthermore, we elaborated general synthetic methodology for the assembly of the *n*-butyl group onto the imidazole ring via the Wittig reaction as well as the bis-alkylation of the N-1 and N-3 of 4(5)-butylimidazole and 2-butylimidazole with the biphenylmethyl moiety. A remarkably efficient approach was also adopted for the introduction of the hydroxymethyl group at the C-2 position, as we have previously shown [19]. The SAR studies demonstrated the importance of the nature and the position of pharmacophores. In particular, the presence of two anionic tetrazole groups along with the lipophilic *n*-butyl group at the C-5 led to the potent analogs **11** and its water soluble salts **12a** and **12b**. The introduction of the electronegative hydroxymethyl group at the C-2 (analog **14**) led to acquisition of affinity and potency, while the presence of a halogen atom at the C-4 of the imidazole ring (analog **19c–e** and **23c–e**) led to an essential decrease in affinity. Therefore,

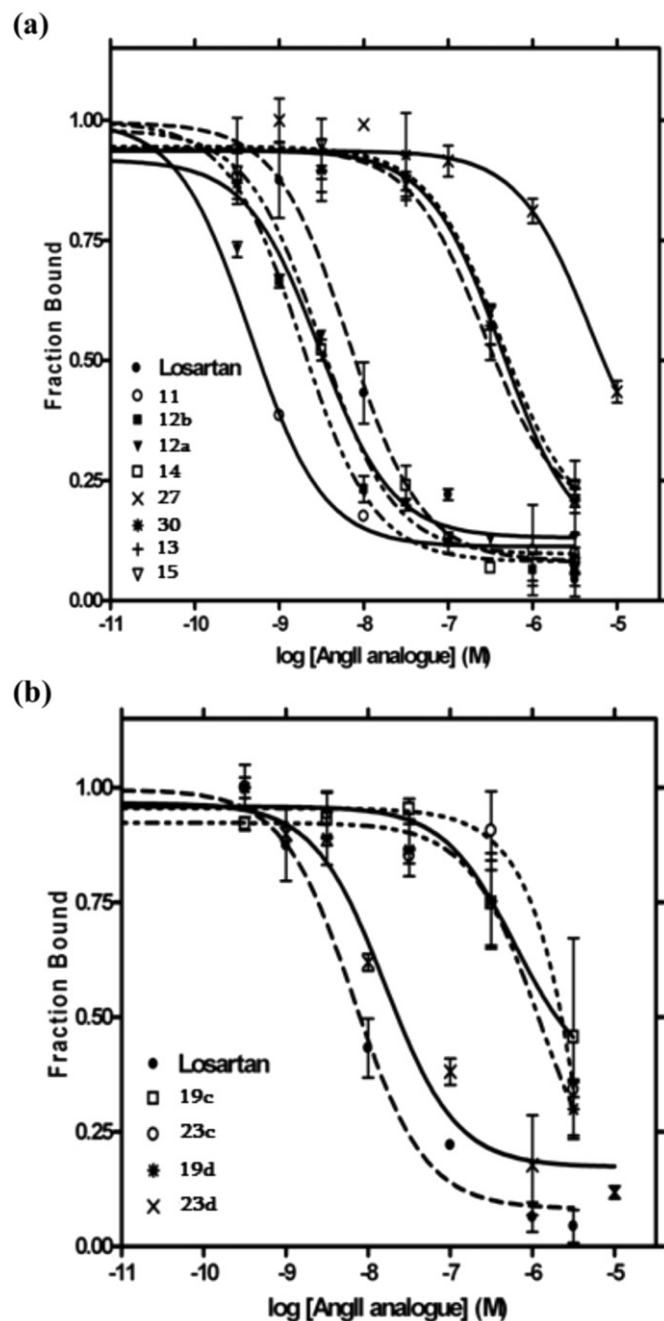


Fig. 12. Competition binding isotherms of ANGII analogs to human AT1 receptor. Competition of [¹²⁵I-Sar¹-Ile⁸] ANGII specific binding by increasing concentrations of ANGII analogs was performed as described under “materials and methods” using membranes from HEK 293 cells stably expressing the human AT1 receptor. The means and S.E. are shown from 2 to 4 different experiments. The data were fit to a one-site competition model by nonlinear regression and the -logIC₅₀ values were determined as described under “materials and methods”. (a) Losartan and analogs **11**, **12a**, **12b**, **13**, **14**, **15**, **27** and **30** (b) Losartan and analogs **19c**, **19d**, **23c** and **23d**.

the presence of two tetrazole rings seems to be optimal for high affinity in contrast to the carboxy group (analog **13**, **15**) which represents poor bioisostere for the tetrazole group, since these analogs showed remarkably low affinity. The position of the *n*-butyl group plays a significant role, since reorientation from the 4- (analog **11**, **12a**, **12b**) to the 2-position (**27**, **30**) of the imidazole ring resulted in a sharp drop of binding affinity. This dramatic loss of activity may be explained by the concealment of the *n*-butyl group between the two biphenyltetrazole moieties.

Of paramount importance were the biological results of the synthetic analog **12b**. Its higher affinity and potency to antagonize ANGII compared to Losartan can be explained by docking studies which demonstrated an additional hydrophobic cavity. MD calculations on lipid bilayers showed that this molecule is incorporated at the interface and exerts a network of interactions with polar region. Thus, this molecule does not only interact with the same binding site as other sartans but also acts through lipid bilayer at the same topographical location [41–44]. Particularly, it anchors at the interface as other sartans where exerts its amphiphilic interactions both with the polar region and upper hydrophobic segments of the phospholipid bilayers. Biophysical studies are in progress to provide more information on this issue. Another important finding from these studies is the critical role of the orientation of the lipophilic *n*-butyl group. The highly hydrophobic residues of receptor that surround this group and interact through van der Waals interactions can explain its orientation significance.

4. Experimental section

4.1. Chemistry

4.1.1. General

Starting materials were obtained by Aldrich and used as received. All reactions involving air sensitive reagents were performed under Ar atmosphere using syringe-septum cap techniques. Melting points were determined with a Stuart SMP 10 apparatus and are uncorrected. Hydrogenation reaction was carried out in a Parr Hydrogenation Apparatus equipped with a 4 L Hydrogen tank. ¹H NMR and ¹³C NMR spectra were recorded on a Bruker Avance DPX spectrometer at 400.13 MHz and 161.76 MHz, respectively. Chemical shifts are reported in units, parts per million (ppm) downfield from tetramethylsilane (TMS) and coupling constants (*J*) are given in Hertz (Hz). The 2D DQF-COSY and ROESY NMR spectra were recorded on a Varian DirectDrive 800 MHz spectrometer at 25 °C. 2 mg of **12b** were dissolved in 0.7 mL of D₂O. Experiments were recorded in the phase-sensitive mode using the pulse sequences in the Varian library of pulse programs. Spectra were acquired with a spectral width of 8012 Hz, 4096 data points in *t*₂, 4–32 scans, 512 complex points in *t*₁, and a relaxation delay of 1.5 s. The mixing time in 2D ROESY was 75 ms. HPLC analysis was performed on an Alliance Waters 2695 equipped with a Waters 2996 Photodiode Array Detector UV–vis, using the XBridge C18 column (4.6 × 150 mm, 3.5 μm) as stationary phase and a gradient of H₂O/MeCN both containing 0.08% TFA as mobile phase. Electrospray ionization mass spectra (ESI-MS) were obtained on a UPLC (ultra performance liquid chromatography) equipped with SQ detector Acquity™ by Waters. All reactions were carried out in anhydrous solvents. Analytical TLC was performed on silica gel 60 F₂₅₄ plates (Merck, Germany) and visualized by UV irradiation and iodine.

4.2. Synthesis of 4(5)-butylimidazole (**5a**)

4.2.1. 1-Trityl-imidazole-4-carboxaldehyde (**2a**)

Prepared from imidazole (**1**) as starting material according to the literature method [20,21]. Data are consistent with literature. *R*_f 0.53 (EtOAc/Hex 4:1); *t*_R 11.59 min (30% MeCN → 100% MeCN in 30 min); ¹H NMR (400 MHz, CDCl₃): δ 9.88 (s, 1H), 7.61 (d, 1H, *J* = 1.3 Hz), 7.53 (s, 1H, *J* = 1.3 Hz), 7.38–7.36 (m, 9H), 7.12–7.10 (m, 6H); ¹³C NMR (160 MHz, CDCl₃): δ 186.51, 141.47, 140.79, 140.56, 129.60, 128.49, 128.34, 127.88, 126.72.

4.2.2. (*Z*)-1-Trityl-4-(but-1-enyl)imidazole (**3a**)

A suspension of **2a** (0.50 g, 1.48 mmol), propyl triphenylphosphonium bromide (0.63 g, 1.63 mmol) and NaH (powered 95%, 0.05 g,

2.22 mmol) in anhydrous THF (8 mL), was stirred at rt for 8 h under Ar atmosphere. Then, the reaction mixture was quenched with saturated aqueous NaHCO₃ (5 mL) solution and extracted with CH₂Cl₂ (3 × 15 mL). The organic layer was washed with H₂O (1 × 10 mL), dried over Na₂SO₄ and concentrated in vacuo. The residue was purified by flash column chromatography (silica gel, EtOAc/Hex 1:1) to furnish the *Z*-**3** isomer (0.44 g) which is the sole isolated product. Yield: 81%; *R*_f 0.63 (EtOAc/Hex 4:1); *t*_R 12.42 min (30% MeCN → 100% MeCN in 30 min); ESI-MS (*m/z*): 123.18 [M + H], 243.26 [Tr]; ¹H NMR (400 MHz, CDCl₃): δ 7.64 (br s, 1H), 7.36–7.35 (m, 9H), 7.16–7.13 (m, 6H), 6.75 (br s, 1H), 6.25 (dt, 1H, *J* = 1.5, 11.6 Hz), 5.60 (dt, 1H, *J* = 7.5, 11.6 Hz), 2.28 (quint d, 2H, *J* = 1.7, 7.5 Hz), 1.00 (t, 3H, *J* = 7.5 Hz); ¹³C NMR (160 MHz, CDCl₃): δ 141.70, 137.64, 137.15, 134.53, 129.66, 128.29, 128.18, 120.20, 119.00, 76.03, 22.55, 13.79.

4.2.3. 1-Trityl-4-butylimidazole (**4a**)

A solution of **3a** (0.30 g, 0.82 mmol) in anhydrous MeOH (10 mL) was transferred in a hydrogenation flask and Pd/C (10% wt/wt, 0.04 g, 0.04 mmol) was added. The reaction mixture was allowed to proceed at rt, under a H₂ atmosphere at a pressure of 3 bar (Parr hydrogenator apparatus) for 2 h. Then, the catalyst was filtered through a pad of Celite® and washed with MeOH. The combined filtrates were concentrated in vacuo to furnish **4a** as a white foam (0.28 g), which was directly used without further purification. Yield: 92%; *R*_f 0.53 (EtOAc/Hex 4:1); *t*_R 13.15 min (30% MeCN → 100% MeCN in 30 min); ESI-MS (*m/z*): 367.50 [M + H], 243.38 [Tr]; ¹H NMR (400 MHz, CDCl₃): δ 7.64 (s, 1H), 7.33–7.31 (m, 10H), 7.15–7.13 (m, 6H), 6.50 (s, 1H), 2.53 (t, 2H, *J* = 7.5 Hz), 1.59 (q, 2H, *J* = 7.5 Hz), 1.33 (sext, 2H, *J* = 7.5 Hz), 0.91 (t, 3H, *J* = 7.5 Hz); ¹³C NMR (160 MHz, CDCl₃): δ 148.81, 142.63, 142.12, 138.16, 129.79, 127.93, 127.89, 127.85, 127.15, 117.60, 74.99, 31.48, 28.17, 22.41, 13.91.

4.2.4. 4(5)-Butylimidazole (**5a**)

Compound **4a** (0.20 g, 0.55 mmol) was dissolved in a solution of 20% TFA in CH₂Cl₂ (2 mL) and then Et₃SiH (0.09 mL, 0.55 mmol) was added as scavenger. The resulting solution was stirred at rt for 1 h and concentrated in vacuo. Precipitation from Et₂O furnished the TFA salt of **5a** as an amorphous powder. The TFA salt was neutralized by treatment with saturated aqueous NaHCO₃ solution for 30 min at rt and extracted with CH₂Cl₂ (3 × 10 mL). The organic phase was dried over Na₂SO₄, filtered and concentrated in vacuo to afford **5a** (0.06 g) as a yellow solid. Yield: 87%; m.p. 45–47 °C; *R*_f 0.60 (CHCl₃/MeOH 9:1); *t*_R 6.82 min (5% MeCN → 100% MeCN in 30 min); ESI-MS (*m/z*): 125.19 [M + H]; ¹H NMR (400 MHz, CD₃OD): δ 7.54 (s, 1H), 6.74 (s, 1H), 2.59 (t, 2H, *J* = 7.2 Hz), 1.62 (quint, 2H, *J* = 7.2 Hz), 1.38 (sext, 2H, *J* = 7.2 Hz), 0.97 (t, 3H, *J* = 7.2 Hz); ¹³C NMR (160 MHz, CD₃OD): δ 136.83, 134.47, 117.28, 31.76, 26.04, 22.28, 13.17.

4.3. Synthesis of 2-butylimidazole (**5b**), method A

4.3.1. 1-[(*N,N*-Dimethylamino)methyl]imidazole (**2b**)

Prepared from imidazole (**1**) according to the literature method [23]. Data were consistent with literature. *R*_f 0.44 (CHCl₃/MeOH 9:1); *t*_R 2.41 min (5% MeCN → 100% MeCN in 30 min); ESI-MS (*m/z*): 126.58 [M + H]; ¹H NMR (400 MHz, CDCl₃): δ 7.44 (s, 1H), 7.01 (s, 1H), 6.90 (s, 1H), 4.61 (s, 2H), 2.23 (s, 6H); ¹³C NMR (160 MHz, CDCl₃): δ 137.63, 129.08, 119.74, 69.25, 41.49.

4.3.2. 2-Butylimidazole (**5b**)

To a solution of **2b** (0.25 g, 2 mmol) in anhydrous THF (10 mL) under Ar atmosphere was added *n*-BuLi (1.6 M in hexanes, 1.37 mL, 2.20 mmol) dropwise via a syringe at –78 °C. After 30 min, DMPU (0.48 mL, 4.0 mmol) was added at –70 °C and stirred for additional 30 min before *n*-BuI (0.27 mL, 2.40 mmol) was added at –78 °C. The reaction mixture was allowed to warm to rt over a period of 16 h.

Then, aqueous HCl (2 M, 8 mL) was added, the organic solvent was removed and the resulting mixture was neutralized with saturated aqueous NaHCO₃ solution and extracted with CH₂Cl₂ (3 × 15 mL). The organic phase was dried over Na₂SO₄ and concentrated in vacuo to furnish **5b** as a pale yellow oil (0.21 g). Data were consistent with literature. Yield: 85%; *R_f* 0.54 (CHCl₃/MeOH 9:1); *t_R* 5.52 min (5% MeCN → 100% MeCN in 30 min); ESI-MS (*m/z*): 125.17 [M + H]⁺; ¹H NMR (400 MHz, CDCl₃): δ 6.87 (s, 2H), 2.68 (t, 2H, *J* = 7.5 Hz), 1.67 (quint, 2H, *J* = 7.5 Hz), 1.34 (sext, 2H, *J* = 7.5 Hz), 0.93 (t, 3H, *J* = 7.5 Hz); ¹³C NMR (160 MHz, CDCl₃): δ 148.97, 120.84, 30.81, 27.64, 22.20, 12.95.

4.4. Synthesis of 2-butylimidazole (**5b**), method B

4.4.1. 1-(*N,N*-Dimethylsulfamoyl)imidazole-2-carboxaldehyde (**2c**)

Prepared from imidazole (**1**) according to the literature method [25]. Data are consistent with literature. *R_f* 0.20 (EtOAc/Hex 7:3); *t_R* 5.00 min (5% MeCN → 100% MeCN in 30 min); ESI-MS (*m/z*): 204.29 [M + H]⁺; ¹H NMR (400 MHz, CDCl₃): δ 9.93 (s, 1H), 7.58 (d, 1H, *J* = 1.5 Hz), 7.30 (d, 1H, *J* = 1.5 Hz), 3.00 (s, 6H); ¹³C NMR (160 MHz, CDCl₃): δ 179.09, 143.45, 130.16, 125.87, 38.56.

4.4.2. 1-(*N,N*-Dimethylsulfamoyl)-2-(but-1-enyl)imidazole (**3c**)

To a stirred suspension of propyl triphenylphosphonium bromide (1.43 g, 3.72 mmol) and anhydrous *t*-amyl alcohol (0.45 mL, 4.09 mmol) in anhydrous THF (14 mL) was added NaH (powdered 95%, 0.10 g, 4.09 mmol) at 0 °C under Ar atmosphere and stirred at rt for 2 h. To the resulting yellow phosphorous ylide was added a solution of **2c** (0.38 g, 1.86 mmol) in anhydrous THF (2 mL) dropwise at 0 °C. The mixture was stirred at rt over a period of 8 h before being quenched with saturated aqueous NaHCO₃ solution and extracted with CH₂Cl₂ (3 × 20 mL). The organic layer was washed with H₂O (2 × 10 mL), dried over Na₂SO₄ and concentrated in vacuo. The residue was purified by flash column chromatography (silica gel, EtOAc/Hex 3:2) to afford the pure *Z*- and *E*-**9** isomers as yellow oils (0.26 g and 0.10 g, respectively). *Z*-Isomer: yield: 62%; *R_f* 0.46 (EtOAc/Hex 7:3); *t_R* 10.08 min (5% MeCN → 100% MeCN in 30 min); ESI-MS (*m/z*): 230.33 [M + H]⁺; ¹H NMR (400 MHz, CDCl₃): δ 7.27 (d, 1H, *J* = 1.3 Hz), 7.07 (d, 1H, *J* = 1.3 Hz), 6.66 (dt, 1H, *J* = 1.3, 11.7 Hz), 5.98 (dt, 1H, *J* = 7.4, 11.7 Hz), 2.85 (s, 6H), 2.70 (quint d, 2H, *J* = 1.9, 7.4 Hz), 1.08 (t, 3H, *J* = 7.4 Hz); ¹³C NMR (160 MHz, CDCl₃): δ 145.14, 142.46, 128.00, 119.69, 114.76, 38.37, 22.86, 13.73. *E*-Isomer: yield: 24%; *R_f* 0.25 (EtOAc/Hex 7:3); *t_R* 10.26 min (5% MeCN → 100% MeCN in 30 min); ESI-MS (*m/z*): 230.29 [M + H]⁺; ¹H NMR (400 MHz, CDCl₃): δ 7.25 (d, 1H, *J* = 1.5 Hz), 6.99 (s, 1H, *J* = 1.5 Hz), 6.90 (dt, 1H, *J* = 7.4, 15.6 Hz), 6.78 (d, 1H, *J* = 15.6 Hz), 2.85 (s, 6H), 2.82 (quint d, 2H, *J* = 1.4, 7.4 Hz), 1.10 (t, 3H, *J* = 7.4 Hz); ¹³C NMR (160 MHz, CDCl₃): δ 146.38, 141.41, 128.06, 119.89, 115.86, 38.33, 26.00, 12.91.

4.4.3. 1-(*N,N*-Dimethylsulfamoyl)-2-butylimidazole (**4c**)

Compound **4c** was prepared in an analogous manner to that described for **4a**. A mixture of the isolated *Z*- and *E*- was subjected to catalytic hydrogenation. Yield: 90%; *R_f* 0.44 (CHCl₃/MeOH 95:5); *t_R* 10.45 min (5% MeCN → 100% MeCN in 30 min); ESI-MS (*m/z*): 231.97 [M + H]⁺; ¹H NMR (400 MHz, CD₃OD): δ 7.38 (d, 1H, *J* = 1.4 Hz), 6.64 (d, 1H, *J* = 1.4 Hz), 3.30 (s, 6H), 2.95 (t, 2H, *J* = 7.6 Hz), 1.73 (quint, 2H, *J* = 7.6 Hz), 1.40 (sext, 2H, *J* = 7.6 Hz), 0.95 (t, 3H, *J* = 7.6 Hz); ¹³C NMR (160 MHz, CD₃OD): δ 144.16, 126.16, 119.66, 37.16, 30.08, 27.68, 21.97, 12.66.

4.4.4. 2-Butylimidazole (**5b**)

A solution of **4c** (0.20 g, 0.86 mmol) in THF (2 mL) was refluxed with 1.5 N HCl (3 mL) for 2 h and then cooled. After neutralization by addition of saturated aqueous NaHCO₃ solution, the solvent was concentrated in vacuo to give a residue, which was extracted with

CH₂Cl₂ (3 × 10 mL). The combined organic extracts were washed with brine, dried over Na₂SO₄ and concentrated in vacuo to afford **7** as a pale yellow oil (0.09 g, 86%).

4.5. General procedure 1: bis-alkylation of 4(5)-butylimidazole (**5a**)

4.5.1. 4-Butyl-*N,N'*-bis[[2'-[2-(trityl)tetrazol-5-yl]biphenyl-4-yl]methyl]imidazolium bromide (**7**)

To a solution of 4(5)-butylimidazole (**5a**) (1.00 g, 8.05 mmol) in anhydrous DMF (30 mL) were sequentially added K₂CO₃ (2.22 g, 16.10 mmol) and the alkylating agent **6a** (10.31 g, 18.52 mmol) under Ar atmosphere and stirred at rt for 8 h. Then, the mixture was diluted with CH₂Cl₂ (90 mL), washed with H₂O (3 × 50 mL), the organic phase was dried over Na₂SO₄, filtered and concentrated in vacuo. The resulting residue was precipitated from cold Et₂O to afford **7** as a white solid. Yield 78%; *R_f* 0.45 (CHCl₃/MeOH, 9:1); *t_R* 15.93 min (70% MeCN → 100% MeCN in 30 min); ESI-MS (*m/z*): 1078.56 [M – Br], 243.17 [Tr]; ¹H NMR (400 MHz, CDCl₃): δ 11.03 (s, 1H), 7.90–7.84 (m, 2H), 7.43–7.30 (m, 5H), 7.30–7.09 (m, 25H), 6.88–6.83 (m, 14H), 6.46 (s, 1H), 5.31 (s, 4H), 2.20 (t, 2H, *J* = 7.5 Hz), 1.26–1.09 (m, 4H), 0.72 (t, 3H, *J* = 7.5 Hz).

4.5.2. 4-Butyl-*N,N'*-bis[[2'-(*tert*-butoxycarbonyl)biphenyl-4-yl]methyl]imidazolium bromide (**8**)

The same procedure was employed for the alkylation of **5a** by treatment with the alkylating agent **6b**. Yield 82%; *R_f* 0.32 (CHCl₃/MeOH 9:1); *t_R* 9.59 min (60% MeCN → 100% MeCN in 30 min); ESI-MS (*m/z*): 657.63 [M – Br]; ¹H NMR (400 MHz, CDCl₃): δ 11.02 (s, 1H), 7.80 (dd, 2H, *J* = 7.5 Hz, *J* = 1.2 Hz), 7.47 (t, 2H, *J* = 7.6 Hz), 7.40 (t, 2H, *J* = 7.6 Hz), 7.35–7.22 (m, 8H), 7.11 (d, 2H, *J* = 7.5 Hz), 6.79 (s, 1H), 5.56 (s, 2H), 5.50 (s, 2H), 2.43 (t, 2H, *J* = 7.4 Hz), 1.44 (quint, 2H, *J* = 7.4 Hz), 1.30 (sext, 2H, *J* = 7.4 Hz), 1.21 (s, 18H), 0.82 (t, 3H, *J* = 7.4 Hz).

4.6. General procedure 2: hydroxymethylation at C-2 position of **7**

4.6.1. 4-Butyl-2-hydroxymethyl-*N,N'*-bis[[2'-[2-(trityl)tetrazol-5-yl]biphenyl-4-yl]methyl]imidazolium bromide (**9**)

In a sealed tube were sequentially added **7** (0.50 g, 0.43 mmol), DMF (1 mL), 37% formalin (0.11 mL, 1.48 mmol) and diisopropylethylamine (0.51 mL, 3.01 mmol). The resulting mixture was stirred at 80 °C until HPLC showed no starting material left (ca. 1 h). Then, the mixture was diluted with CH₂Cl₂ (30 mL), washed with 5% aqueous citric acid (2 × 10 mL), brine (×10 mL), the organic phase was dried over Na₂SO₄, filtered and concentrated in vacuo. The resulting residue was precipitated from cold Et₂O to afford **9** as a white powder. Yield 84%; *R_f* 0.36 (CHCl₃/MeOH 9:1); *t_R* 15.32 min (70% MeCN → 100% MeCN in 30 min); ESI-MS (*m/z*): 1108.06 [M – Br]; ¹H NMR (400 MHz, CDCl₃): δ 7.96–7.93 (m, 2H), 7.50–7.43 (m, 5H), 7.37–7.14 (m, 20H), 7.07 (d, 2H, *J* = 8.0 Hz), 6.94–6.91 (m, 15H), 6.85 (d, 2H, *J* = 8.0 Hz), 6.46 (s, 1H), 5.53 (s, 2H), 5.47 (s, 2H), 4.64 (s, 2H), 2.34 (t, 2H, *J* = 7.5 Hz), 1.40 (quint, 2H, *J* = 7.5 Hz), 1.26 (sext, 2H, *J* = 7.5 Hz), 0.80 (t, 3H, *J* = 7.5 Hz).

4.6.2. 4-Butyl-2-hydroxymethyl-*N,N'*-bis[[2'-(*tert*-butoxycarbonyl)]biphenyl-4-yl]methyl]imidazolium bromide (**10**)

The same procedure was employed for the hydroxymethylation of **8**. Yield: 81%; *R_f* 0.31 (CHCl₃/MeOH 9:1); *t_R* 8.91 min (60% MeCN → 100% MeCN in 30 min); ESI-MS (*m/z*): 687.56 [M – Br]; ¹H NMR (400 MHz, CDCl₃): δ 7.72 (t, 2H, *J* = 7.0 Hz), 7.47–7.40 (m, 2H), 7.36–7.17 (m, 10H), 7.04 (d, 2H, *J* = 8.0 Hz), 6.85 (s, 1H), 5.66 (s, 4H), 4.82 (s, 2H), 2.48 (t, 2H, *J* = 7.5 Hz), 1.49 (quint, 2H, *J* = 7.5 Hz), 1.31 (sext, 2H, *J* = 7.5 Hz), 1.21 (s, 9H), 1.20 (s, 9H), 0.83 (t, 3H, *J* = 7.5 Hz).

4.7. General procedure 3: removal of protective groups

4.7.1. 4-Butyl-*N,N'*-bis[[2'-(2H-tetrazol-5-yl)]biphenyl-4-yl]methyl]imidazolium bromide (**11**)

Compound **7** (0.40 g, 0.34 mmol) was dissolved in a solution of 30% TFA (1.2 mL) in CH₂Cl₂ (2.8 mL) and then Et₃SiH (54 μL, 0.34 mmol) was added as a scavenger. The resulting solution was stirred at rt for 1 h before being concentrated in vacuo. Precipitation from Et₂O furnished an amorphous solid, then, dissolved in CH₂Cl₂ (20 mL) and the resulting mixture was washed with saturated aqueous NaHCO₃ solution (2 × 5 mL), dried over Na₂SO₄, filtered and concentrated in vacuo to furnish **11** as a white solid: yield 72%; m.p. 201–203 °C; *R*_f 0.35 (CHCl₃/MeOH/gl. AcOH, 9:1:0.1); *t*_R 12.35 min (20% MeCN → 100% MeCN in 30 min); ESI-MS (*m/z*): 593.57 [M – Br]; ¹H NMR (400 MHz, DMSO-*d*₆): δ 9.35 (d, 1H, *J* = 1.2 Hz), 7.71–7.67 (m, 4H), 7.62 (d, 2H, *J* = 7.0 Hz), 7.59 (br s, 1H), 7.55 (d, 2H, *J* = 7.0 Hz), 7.37 (d, 2H, *J* = 8.1 Hz), 7.25 (d, 2H, *J* = 8.1 Hz), 7.19–7.16 (m, 4H), 5.45 (s, 2H), 5.41 (s, 2H), 1.44 (quint, 2H, *J* = 7.5 Hz), 1.28 (sext, 2H, *J* = 7.5 Hz), 0.94 (t, 3H, *J* = 7.5 Hz); ¹³C NMR (160 MHz, CD₃OD): δ 9.02 (br s, 1H), 7.71–7.67 (m, 4H), 7.61–7.56 (m, 4H), 7.46 (br s, 1H), 7.36 (d, 2H, *J* = 8.0 Hz), 7.26–7.20 (m, 6H), 5.40 (s, 2H), 5.38 (s, 2H), 2.57 (t, 2H, *J* = 7.5 Hz), 1.56 (quint, 2H, *J* = 7.5 Hz), 1.38 (sext, 2H, *J* = 7.5 Hz), 0.92 (t, 3H, *J* = 7.5 Hz); ¹³C NMR (160 MHz, DMSO-*d*₆): δ 160.54, 160.19, 143.46, 142.99, 142.92, 138.99, 138.29, 136.00, 135.48, 133.30, 133.26, 133.10, 133.02, 132.30, 132.26, 132.22, 132.03, 130.57, 130.47, 130.29, 130.22, 130.12, 129.99, 122.21, 54.46, 51.98, 31.30, 25.27, 24.24, 16.25.

4.8. General procedure 4: conversion to the potassium salt **12a**

4.8.1. Bis-potassium salt of 4-butyl-*N,N'*-bis[[2'-(2H-tetrazol-5-yl)]biphenyl-4-yl]methyl]imidazolium bromide (**12a**)

To a suspension of **11** (0.20 g, 0.30 mmol) in MeOH–H₂O, 1:1 (4 mL) was added KOH (33 mg, 0.60 mmol) and the reaction mixture was stirred at rt for 5 h. Activated charcoal was added to the mixture, stirred for 10 min before being filtered through a pad of Celite®. The filtrate was concentrated in vacuo to remove ca. half the solvent volume. The residue was precipitated with acetone to afford a white solid. Lyophilization of the resulting solid furnished the potassium salt **12a** as a white foam. Yield 80%; *R*_f 0.30 (CHCl₃/MeOH/gl. AcOH, 9:1:0.1); *t*_R 12.19 min (20% MeCN → 100% MeCN in 30 min); ESI-MS (*m/z*): 631.23 [(M – K) + H – Br]; ¹H NMR (400 MHz, CD₃OD): δ 8.93 (s, 1H), 7.60–7.58 (m, 2H), 7.53–7.50 (m, 2H), 7.47–7.45 (m, 4H), 7.41 (s, 1H), 7.27 (d, 2H, *J* = 8.0 Hz), 7.21–7.15 (m, 6H), 5.33 (s, 2H), 5.32 (s, 2H), 2.59 (t, 2H, *J* = 7.5 Hz), 1.56 (quint, 2H, *J* = 7.5 Hz), 1.39 (sext, 2H, *J* = 7.5 Hz), 0.93 (t, 3H, *J* = 7.5 Hz); ¹³C NMR (160 MHz, CD₃OD): δ 161.22, 161.21, 144.27, 142.15, 143.16, 140.86, 140.82, 136.61, 131.93, 130.52, 130.50, 129.95, 129.88, 129.81, 129.73, 129.69, 128.75, 128.55, 127.62, 127.27, 127.19, 126.94, 119.25, 52.40, 49.89, 28.86, 22.86, 21.74, 12.58.

4.8.2. Bis-sodium salt of 4-butyl-*N,N'*-bis[[2'-(2H-tetrazol-5-yl)]biphenyl-4-yl]methyl]imidazolium bromide (**12b**)

The same procedure was employed for the preparation of sodium salt **12b**. Yield 83%; *t*_R 12.21 min (20% MeCN → 100% MeCN in 30 min); ESI-MS (*m/z*): 615.12 [(M – Na) + H – Br]; ¹H NMR (400 MHz, CD₃OD): δ 8.56 (s, 1H), 7.60–7.58 (m, 2H), 7.55–7.50 (m, 2H), 7.47–7.45 (m, 4H), 7.42 (s, 1H), 7.26 (d, 2H, *J* = 8.2 Hz), 7.19–7.16 (m, 6H), 5.32 (s, 2H), 5.31 (s, 2H), 2.58 (t, 2H, *J* = 7.4 Hz), 1.57 (quint, 2H, *J* = 7.4 Hz), 1.38 (sext, 2H, *J* = 7.4 Hz), 0.93 (t, 3H, *J* = 7.4 Hz) ppm; ¹³C NMR (160 MHz, CD₃OD): δ 163.52, 144.56, 143.12, 134.25, 133.78, 132.73, 132.17, 132.10, 132.03, 131.98, 130.96, 130.02, 129.50, 129.35, 121.43, 54.68, 52.18, 31.13, 25.15, 24.04, 14.83 ppm.

4.9. 4-Butyl-*N,N'*-bis[[2-carboxybiphenyl-4-yl]methyl]imidazolium bromide (**13**)

General procedure 3 was employed for the preparation of **13**. Yield 79%; *R*_f 0.24 (CHCl₃/MeOH/gl. AcOH, 8:2:0.2); *t*_R 16.38 min (10% MeCN → 100% MeCN in 30 min); ESI-MS (*m/z*): 545.45 [M – Br]; ¹H NMR (400 MHz, CD₃OD): δ 9.09 (s, 1H), 7.87 (d, 2H, *J* = 7.6 Hz), 7.57 (t, 2H, *J* = 7.6 Hz), 7.53 (s, 1H), 7.49–7.34 (m, 12H), 5.46 (s, 2H), 5.44 (s, 2H), 2.65 (t, 2H, *J* = 7.3 Hz), 1.59 (quint, 2H, *J* = 7.3 Hz), 1.40 (sext, 2H, *J* = 7.3 Hz), 0.93 (t, 3H, *J* = 7.3 Hz); ¹³C NMR (160 MHz, CD₃OD): δ 173.38, 144.83, 143.73, 139.69, 138.18, 134.16, 134.58, 133.57, 133.35, 132.72, 131.86, 131.50, 131.45, 130.21, 129.58, 121.68, 54.78, 52.25, 31.19, 25.23, 24.05, 14.81.

4.9.1. 4-Butyl-2-hydroxymethyl-*N,N'*-bis[[2'-(2H-tetrazol-5-yl)]biphenyl-4-yl]methyl]imidazolium bromide (**14**)

General procedure 3 was employed for the preparation of **14**. Yield: 83%; *R*_f 0.29 (CHCl₃/MeOH/gl. AcOH, 9:1:0.1); *t*_R 11.59 min (20% MeCN → 100% MeCN in 30 min); ESI-MS (*m/z*): 623.37 [M – Br]; ¹H NMR (400 MHz, CD₃OD): δ 7.56–7.54 (m, 2H), 7.50–7.47 (m, 2H), 7.44–7.41 (m, 4H), 7.37 (s, 1H), 7.20 (d, 2H, *J* = 8.1 Hz), 7.16–7.13 (m, 4H), 7.00 (d, 2H, *J* = 8.1 Hz), 5.46 (s, 2H), 5.42 (s, 2H), 2.51 (t, 2H, *J* = 7.5 Hz), 1.49 (quint, 2H, *J* = 7.5 Hz), 1.32 (sext, 2H, *J* = 7.5 Hz), 0.86 (t, 3H, *J* = 7.5 Hz); ¹H NMR (400 MHz, DMSO-*d*₆): δ 7.69–7.53 (m, 9H), 7.35 (d, 2H, *J* = 8.0 Hz), 7.17–7.12 (m, 6H), 6.26 (s, 1H), 5.53 (s, 2H), 5.48 (s, 2H), 4.92 (s, 2H), 2.40 (t, 2H, *J* = 7.4 Hz), 1.36 (quint, 2H, *J* = 7.4 Hz), 1.22 (sext, 2H, *J* = 7.4 Hz), 0.79 (t, 3H, *J* = 7.4 Hz); ¹³C NMR (160 MHz, CD₃OD): δ 161.22, 160.00, 145.06, 142.04, 141.62, 140.90, 135.96, 132.11, 132.02, 129.74, 129.71, 129.66, 125.68, 125.63, 119.28, 119.06, 51.38, 51.17, 48.09, 28.82, 23.05, 21.68, 12.54.

4.9.2. 4-Butyl-2-hydroxymethyl-*N,N'*-bis[[2'-carboxybiphenyl-4-yl]methyl]imidazolium bromide (**15**)

General procedure 3 was employed for the preparation of **15**. Yield: 85%; *R*_f 0.22 (CHCl₃/MeOH/gl. AcOH 8:2:0.2); *t*_R 16.01 min (10% MeCN → 100% MeCN in 30 min); ESI-MS (*m/z*): 575.50 [M – Br]; ¹H NMR (400 MHz, CD₃OD): δ 7.86 (t, 2H, *J* = 7.0 Hz), 7.60–7.56 (m, 2H), 7.51 (s, 1H), 7.49–7.35 (m, 10H), 7.24 (d, 2H, *J* = 8.0 Hz), 5.62 (s, 2H), 5.59 (s, 2H), 5.00 (s, 2H), 2.60 (t, 2H, *J* = 7.4 Hz), 1.55 (quint, 2H, *J* = 7.4 Hz), 1.37 (sext, 2H, *J* = 7.4 Hz), 0.89 (t, 3H, *J* = 7.4 Hz); ¹³C NMR (160 MHz, CD₃OD): δ 171.46, 145.12, 142.36, 141.95, 140.76, 140.72, 136.11, 132.99, 132.71, 132.67, 130.44, 130.19, 129.08, 127.47, 127.14, 127.05, 125.97, 119.30, 51.37, 51.24, 28.82, 23.13, 21.73, 12.51.

4.10. General procedure 5: halogenation of 4(5)-butylimidazole

4.10.1. 5-Butyl-4-chloro-1H-imidazole (**16c**)

To a solution of **5a** (1.00 g, 8.05 mmol) in anhydrous DMF (5 mL) was added NCS (1.18 g, 8.86 mmol) in three portions at 0 °C. The reaction mixture was allowed to warm to rt over a period of 2 h before being quenched with H₂O (5 mL) and extracted with CH₂Cl₂ (3 × 20 mL). The combined organic phases were washed with brine, dried over Na₂SO₄, filtered and concentrated in vacuo. The oily residue was purified by flash column chromatography (silica gel, CHCl₃/MeOH 95:5) to afford the title compound **16c** as a white solid. Yield: 73%; m.p. 103–105 °C; *R*_f 0.21 (CHCl₃/MeOH, 95:5); *t*_R 8.82 min (5% MeCN → 100% MeCN in 30 min); ESI-MS (*m/z*): 159.16 [M + H] (³⁵Cl), 161.11 [M + H + 2] (³⁷Cl); ¹H NMR (400 MHz, CD₃OD): δ 7.44 (s, 1H), 2.68 (t, 2H, *J* = 7.5 Hz), 1.66 (quint, 2H, *J* = 7.5 Hz), 1.46 (sext, 2H, *J* = 7.5 Hz), 0.93 (t, 3H, *J* = 7.5 Hz); ¹³C NMR (160 MHz, CD₃OD): δ 133.04, 126.14, 124.24, 31.05, 23.23, 22.0, 12.98.

4.10.2. 4-Bromo-5-butyl-1H-imidazole (**16d**)

The same procedure was employed for the preparation of **16d**. Yield: 71%; m.p. 109–111 °C; *R*_f 0.21 (CHCl₃/MeOH/95:5); *t*_R

8.42 min (5% MeCN → 100% MeCN in 30 min); ESI-MS (m/z): 203.15 [M + H] (^{79}Br), 205.11 [M + H + 2] (^{81}Br); ^1H NMR (400 MHz, CD_3OD): δ 2.48 (t, 2H, $J = 7.5$ Hz), 1.50 (quint, 2H, $J = 7.5$ Hz), 1.27 (sext, 2H, $J = 7.5$ Hz), 0.88 (t, 3H, $J = 7.5$ Hz); ^{13}C NMR (160 MHz, CD_3OD): δ 137.91, 132.64, 114.53, 34.66, 27.43, 25.56, 16.58.

4.10.3. 5-Butyl-4-iodo-1H-imidazole (**16e**)

The same procedure was employed for the preparation of **16e**. Yield: 72%; m.p. 93–95 °C; R_f 0.21 ($\text{CHCl}_3/\text{MeOH}/95:5$); t_R 8.94 min (5% MeCN → 100% MeCN in 30 min); ESI-MS (m/z): 250.85 [M + H], 500.80 [2M + H]; ^1H NMR (400 MHz, CD_3OD): δ 7.73 (s, 1H), 2.59 (t, 2H, $J = 7.5$ Hz), 1.60 (quint, 2H, $J = 7.5$ Hz), 1.35 (sext, 2H, $J = 7.5$ Hz), 0.96 (t, 3H, $J = 7.5$ Hz); ^{13}C NMR (160 MHz, CD_3OD): δ 140.56, 137.92, 81.92, 34.98, 28.90, 25.62, 16.72.

4.11. General procedure 6: bis-alkylation of **16c–e** with the alkylating agent **6a**

4.11.1. 5-Butyl-4-chloro-*N,N'*-bis[2'-(trityl)tetrazol-5-yl]biphenyl-4-yl)methyl]imidazolium bromide (**17c**)

To a solution of **16c** (0.20 g, 1.26 mmol) in anhydrous THF (5 mL) under Ar atmosphere were sequentially added anhydrous K_2CO_3 (0.34 g, 2.50 mmol), a catalytic amount of 18-crown-6-ether as a phase transfer catalyst and the alkylating agent **6a** (1.61 g, 2.89 mol). The reaction mixture was stirred under reflux over a period of 12 h before being quenched with H_2O (10 mL) and extracted with CH_2Cl_2 (3×20 mL). The combined organic extracts were dried over Na_2SO_4 , filtered and concentrated in vacuo. Flash column chromatography (silica gel, $\text{CHCl}_3/\text{MeOH}$ 98:2) afforded **17c** as a yellow foam. Yield: 57%; R_f 0.49 ($\text{CHCl}_3/\text{MeOH}/9:1$); t_R 16.81 min (70% MeCN → 100% MeCN in 30 min); ESI-MS (m/z): 1111.82 [M – Br]; ^1H NMR (400 MHz, CDCl_3): δ 11.46 (s, 1H), 7.95–7.93 (m, H), 7.33–7.14 (m, 32H), 6.93–6.90 (m, 12H), 5.44 (s, 2H), 5.42 (s, 2H), 2.37 (t, 2H, $J = 7.5$ Hz), 1.28–1.19 (m, 4H), 0.82 (t, 3H, $J = 7.5$ Hz).

4.11.2. 4-Bromo-5-butyl-*N,N'*-bis[2'-(trityl)tetrazol-5-yl]biphenyl-4-yl)methyl]imidazolium bromide (**17d**)

The same procedure as above was employed for the preparation of **17d**. Yield: 55%; R_f 0.50 ($\text{CHCl}_3/\text{MeOH}$ 9:1); t_R 16.90 min (70% MeCN → 100% MeCN in 30 min); ESI-MS (m/z): 1157.11 [M – Br]; ^1H NMR (400 MHz, CDCl_3): δ 11.28 (s, 1H), 7.89–7.64 (m, 2H), 7.42–7.09 (m, 32H), 6.86–6.84 (m, 12H), 5.38 (s, 4H), 2.33 (t, 2H, $J = 7.5$ Hz), 1.49–1.17 (m, 4H), 0.94 (t, 3H, $J = 7.5$ Hz).

4.11.3. 5-Butyl-4-iodo-*N,N'*-bis[2'-(trityl)tetrazol-5-yl]biphenyl-4-yl)methyl]imidazolium bromide (**17e**)

The same procedure as above was employed for the preparation of **17e**. Yield: 52%; R_f 0.50 ($\text{CHCl}_3/\text{MeOH}$ 9:1); t_R 16.31 min (70% MeCN → 100% MeCN in 30 min); ESI-MS (m/z): 1203.60 [M – Br]; ^1H NMR (400 MHz, CDCl_3): δ 10.88 (s, 1H), 7.94–7.89 (m, 2H), 7.48–7.15 (m, 32H), 6.92–6.89 (m, 12H), 5.38 (s, 2H), 5.36 (s, 2H), 2.60 (t, 2H, $J = 7.5$ Hz), 1.56–1.19 (m, 4H), 0.83 (t, 3H, $J = 7.5$ Hz).

4.12. General procedure 7: bis-alkylation of **16c–e** with the alkylating agent **6b**

4.12.1. 5-Butyl-4-chloro-*N,N'*-bis[2'-(tert-butoxycarbonyl)biphenyl-4-yl)methyl]imidazolium bromide (**18c**)

To a solution of **16c** (0.20 g, 1.26 mmol) in anhydrous Tol (4 mL) under Ar atmosphere were sequentially added powdered KOH (0.14 g, 2.52 mmol), a catalytic amount of 18-crown-6-ether as a phase transfer catalyst and the alkylating agent **6b** (1.00 g, 2.90 mol). The reaction mixture was stirred at 80 °C over a period of 12 h before being quenched with H_2O (10 mL) and extracted with

CH_2Cl_2 (3×20 mL). The combined organic extracts were dried over Na_2SO_4 , filtered and concentrated in vacuo. Flash column chromatography (silica gel, $\text{CHCl}_3/\text{MeOH}$ 97:3) afforded **18c** as a yellow foam. Yield: 61%; R_f 0.35 ($\text{CHCl}_3/\text{MeOH}$ 9:1); t_R 11.52 min (60% MeCN → 100% MeCN in 30 min); ESI-MS (m/z): 691.53 [M – Br] (^{35}Cl), 693.54 [M + 2 – Br] (^{37}Cl); ^1H NMR (400 MHz, CDCl_3): δ 11.46 (s, 1H), 7.73 (d, 2H, $J = 7.6$ Hz), 7.50 (d, 2H, $J = 8.0$ Hz), 7.43–7.28 (m, 8H), 7.21–7.16 (m, 4H), 5.60 (s, 2H), 5.57 (s, 2H), 2.52 (t, 2H, $J = 7.5$ Hz), 1.35–1.24 (m, 4H), 1.20 (s, 9H), 1.17 (s, 9H), 0.82 (t, 3H, $J = 7.5$ Hz).

4.12.2. 4-Bromo-5-butyl-*N,N'*-bis[2'-(tert-butoxycarbonyl)biphenyl-4-yl)methyl]imidazolium bromide (**18d**)

The same procedure as above was employed for the preparation of **18d**. Yield: 64%; R_f 0.36 ($\text{CHCl}_3/\text{MeOH}$ 9:1); t_R 11.34 min (60% MeCN → 100% MeCN in 30 min); ESI-MS (m/z): 736.45 [M – Br] (^{79}Br), 738.51 [M + 2 – Br] (^{81}Br); ^1H NMR (400 MHz, CDCl_3): δ 11.46 (s, 1H), 7.72 (d, 2H, $J = 7.5$ Hz), 7.48 (d, 2H, $J = 8.0$ Hz), 7.41–7.27 (m, 8H), 7.21–7.16 (m, 4H), 5.59 (s, 2H), 5.56 (s, 2H), 2.54 (t, 2H, $J = 7.5$ Hz), 1.37–1.25 (m, 4H), 1.22 (s, 9H), 1.18 (s, 9H), 0.84 (t, 3H, $J = 7.5$ Hz).

4.12.3. 5-Butyl-4-iodo-*N,N'*-bis[2'-(tert-butoxycarbonyl)biphenyl-4-yl)methyl]imidazolium bromide (**18e**)

The same procedure as above was employed for the preparation of **18e**. Yield: 58%; R_f 0.36 ($\text{CHCl}_3/\text{MeOH}$ 9:1); t_R 11.76 min (60% MeCN → 100% MeCN in 30 min); ESI-MS (m/z): 783.43 [M – Br]; ^1H NMR (400 MHz, CDCl_3): δ 11.53 (s, 1H), 7.72 (d, 2H, $J = 7.5$ Hz), 7.51 (d, 2H, $J = 8.0$ Hz), 7.43–7.28 (m, 8H), 7.21–7.16 (m, 4H), 5.59 (s, 4H), 2.51 (t, 2H, $J = 7.4$ Hz), 1.35–1.24 (m, 4H), 1.20 (s, 9H), 1.17 (s, 9H), 0.83 (t, 3H, $J = 7.4$ Hz).

4.13. 5-Butyl-4-chloro-*N,N'*-bis[2'-(2H-tetrazol-5-yl)biphenyl-4-yl)methyl]imidazolium bromide (**19c**)

General procedure 3 was employed for the preparation of **19c**. Yield: 82%; R_f 0.40 ($\text{CHCl}_3/\text{MeOH}/\text{gl. AcOH}$ 9:1:0.1); t_R 13.29 min (20% MeCN → 100% MeCN in 30 min); ESI-MS (m/z): 628.55 [M – Br] (^{35}Cl), 630.50 [M + 2 – Br] (^{37}Cl); ^1H NMR (400 MHz, CD_3OD): δ 9.12 (s, 1H), 7.69–7.66 (m, 4H), 7.60–7.54 (m, 4H), 7.34 (d, 2H, $J = 8.0$ Hz), 7.29 (d, 2H, $J = 8.0$ Hz), 7.23–7.20 (m, 4H), 5.45 (s, 2H), 5.44 (s, 2H), 2.68 (t, 2H, $J = 7.4$ Hz), 1.39–1.30 (m, 4H), 0.87 (t, 3H, $J = 7.4$ Hz); ^{13}C NMR (160 MHz, CD_3OD): δ 156.35, 145.39, 141.54, 141.08, 140.96, 133.99, 132.72, 132.45, 131.52, 131.49, 130.80, 130.60, 130.22, 130.12, 128.55, 128.38, 128.20, 126.69, 123.57, 119.89, 51.55, 51.10, 29.44, 23.21, 22.12, 13.28.

4.13.1. 4-Bromo-5-butyl-*N,N'*-bis[2'-(2H-tetrazol-5-yl)biphenyl-4-yl)methyl]imidazolium bromide (**19d**)

General procedure 3 was employed for the preparation of **19d**. Yield: 80%; R_f 0.43 ($\text{CHCl}_3/\text{MeOH}/\text{gl. AcOH}$ 9:1:0.1); t_R 13.17 min (20% MeCN → 100% MeCN in 30 min); ESI-MS (m/z): 671.37 [M – Br] (^{79}Br), 673.32 [M + 2 – Br] (^{81}Br); ^1H NMR (400 MHz, CD_3OD): δ 9.12 (s, 1H), 7.66–7.63 (m, 4H), 7.57–7.52 (m, 4H), 7.32 (d, 2H, $J = 8.0$ Hz), 7.26–7.19 (m, 4H), 7.07 (d, 2H, $J = 8.0$ Hz), 5.44 (s, 2H), 5.41 (s, 2H), 2.67 (t, 2H, $J = 7.4$ Hz), 1.40–1.30 (m, 4H), 0.88 (t, 3H, $J = 7.4$ Hz); ^{13}C NMR (160 MHz, CD_3OD): δ 156.42, 156.35, 145.33, 141.10, 135.09, 133.58, 132.17, 131.93, 130.62, 130.30, 130.21, 129.85, 128.68, 127.76, 124.18, 106.82, 51.65, 51.04, 29.23, 22.78, 21.77, 13.74.

4.13.2. 5-Butyl-4-iodo-*N,N'*-bis[2'-(2H-tetrazol-5-yl)biphenyl-4-yl)methyl]imidazolium bromide (**19e**)

General procedure 3 was employed for the preparation of **19e**. Yield: 79%; R_f 0.43 ($\text{CHCl}_3/\text{MeOH}/\text{gl. AcOH}$ 9:1:0.1); t_R 13.0 min (20%

MeCN → 100% MeCN in 30 min); ESI-MS (m/z): 719.45 [M – Br]; ^1H NMR (400 MHz, CD_3OD): δ 9.24 (s, 1H), 7.67–7.62 (m, 4H), 7.59–7.53 (m, 4H), 7.30 (d, 2H, $J = 8.0$ Hz), 7.29–7.21 (m, 4H), 7.09 (d, 2H, $J = 8.0$ Hz), 5.50 (s, 2H), 5.43 (s, 2H), 2.70 (t, 2H, $J = 7.5$ Hz), 1.37–1.30 (m, 4H), 0.97 (t, 3H, $J = 7.5$ Hz); ^{13}C NMR (160 MHz, CD_3OD): δ 157.52, 146.43, 140.59, 135.75, 133.49, 133.07, 131.23, 130.72, 130.55, 130.15, 129.93, 129.41, 128.01, 127.56, 126.08, 89.85, 51.80, 50.04, 29.23, 22.78, 21.77, 13.74.

4.13.3. 5-Butyl-4-chloro-*N,N'*-bis[2'-carboxybiphenyl-4-yl]methylimidazolium bromide (**20c**)

General procedure 3 was employed for the preparation of **20c**. Yield: 79%; R_f 0.26 ($\text{CHCl}_3/\text{MeOH}/\text{gl. AcOH}$ 8:2:0.2); t_R 17.35 min (10% MeCN → 100% MeCN in 30 min); ESI-MS (m/z): 579.34 [M – Br] (^{35}Cl), 581.36 [M + 2 – Br] (^{37}Cl); ^1H NMR (400 MHz, CD_3OD): δ 9.14 (s, 1H), 7.82–7.79 (m, 2H), 7.51 (td, 2H, $J = 7.6$ Hz, 1.4 Hz), 7.42–7.28 (m, 12H), 5.44 (s, 2H), 5.43 (s, 2H), 2.68 (t, 2H, $J = 7.5$ Hz), 1.40–1.22 (m, 4H), 0.83 (t, 3H, $J = 7.5$ Hz); ^{13}C NMR (160 MHz, CD_3OD): δ 173.58, 148.32, 145.51, 143.69, 134.57, 132.87, 132.50, 132.35, 131.59, 130.45, 130.17, 129.82, 129.52, 123.91, 54.78, 52.25, 31.19, 25.23, 24.05, 14.81.

4.13.4. 4-Bromo-5-butyl-*N,N'*-bis[2'-carboxybiphenyl-4-yl]methylimidazolium bromide (**20d**)

General procedure 3 was employed for the preparation of **20d**. Yield: 76%; R_f 0.26 ($\text{CHCl}_3/\text{MeOH}/\text{gl. AcOH}$ 8:2:0.2); t_R 17.27 min (10% MeCN → 100% MeCN in 30 min); ESI-MS (m/z): 623.30 [M – Br] (^{79}Br), 625.32 [M + 2 – Br] (^{81}Br); ^1H NMR (400 MHz, CD_3OD): δ 9.24 (s, 1H), 7.81–7.78 (m, 2H), 7.49 (td, 2H, $J = 7.5$ Hz, 1.3 Hz), 7.42–7.27 (m, 12H), 5.46 (s, 2H), 5.39 (s, 2H), 2.67 (t, 2H, $J = 7.4$ Hz), 1.33–1.29 (m, 4H), 0.84 (t, 3H, $J = 7.4$ Hz); ^{13}C NMR (160 MHz, CD_3OD): δ 173.30, 148.38, 145.00, 144.89, 143.18, 137.39, 135.14, 134.32, 133.75, 132.91, 132.55, 131.59, 131.47, 130.12, 129.81, 129.56, 129.52, 109.14, 54.67, 53.52, 31.56, 25.18, 24.16, 14.77.

4.13.5. 5-Butyl-4-iodo-*N,N'*-bis[2'-carboxybiphenyl-4-yl]methylimidazolium bromide (**20e**)

General procedure 3 was employed for the preparation of **20e**. Yield: 73%; R_f 0.26 ($\text{CHCl}_3/\text{MeOH}/\text{gl. AcOH}$ 8:2:0.2); t_R 17.42 min (10% MeCN → 100% MeCN in 30 min); ESI-MS (m/z): 671.31 [M – Br]; ^1H NMR (400 MHz, CD_3OD): δ 9.20 (s, 1H), 7.81–7.79 (m, 2H), 7.50 (td, 2H, $J = 1.2, 7.5$ Hz), 7.42–7.28 (m, 12H), 5.45 (s, 2H), 5.42 (s, 2H), 2.67 (t, 2H, $J = 7.3$ Hz), 1.38–1.23 (m, 4H), 0.83 (t, 3H, $J = 7.3$ Hz); ^{13}C NMR (160 MHz, CD_3OD): δ 173.41, 147.88, 144.86, 144.68, 143.40, 141.99, 134.32, 134.11, 133.08, 132.58, 132.55, 131.53, 131.37, 129.98, 129.64, 129.50, 80.86, 56.12, 53.28, 31.93, 26.47, 24.20, 14.75.

4.14. 5-Butyl-4-chloro-2-hydroxymethyl-*N,N'*-bis[2'-[2-(trityl)tetrazol-5-yl]biphenyl-4-yl]methylimidazolium bromide (**21c**)

General procedure 2 was employed for the preparation of **2c**. Yield: 76%; R_f 0.45 ($\text{CHCl}_3/\text{MeOH}$ 9:1); t_R 16.68 min (70% MeCN → 100% MeCN in 30 min); ESI-MS (m/z): 1141.47 [M – Br], 901.43 [M – Tr] + H – Br], 242.98 [Tr]; ^1H NMR (400 MHz, CDCl_3): δ 7.92–7.86 (m, 2H), 7.47–7.45 (m, 5H), 7.32–7.13 (m, 27H), 6.98–6.71 (m, 12H), 5.76 (s, 2H), 5.67 (s, 2H), 4.73 (s, 2H), 2.51 (t, 2H, $J = 7.5$ Hz), 1.29–1.19 (m, 4H), 0.84 (t, 3H, $J = 7.5$ Hz).

4.14.1. 4-Bromo-5-butyl-2-hydroxymethyl-*N,N'*-bis[2'-[2-(trityl)tetrazol-5-yl]biphenyl-4-yl]methylimidazolium bromide (**21d**)

General procedure 2 was employed for the preparation of **21d**. Yield: 72%; R_f 0.44 ($\text{CHCl}_3/\text{MeOH}$ 9:1); t_R 15.90 min (70% MeCN → 100% MeCN in 30 min); ESI-MS (m/z): 1187.21 [M – Br]; ^1H NMR (400 MHz, CDCl_3) δ 7.91–7.88 (m, 2H), 7.42–7.40 (m, 5H),

7.25–7.08 (m, 27H), 6.86–6.84 (m, 12H), 5.51 (s, 2H), 4.44 (s, 2H), 2.46 (t, 2H, $J = 7.5$ Hz), 1.21–1.19 (m, 4H), 0.79 (t, 3H, $J = 7.5$ Hz).

4.14.2. 5-Butyl-2-hydroxymethyl-4-iodo-*N,N'*-bis[2'-[2-(trityl)tetrazol-5-yl]biphenyl-4-yl]methylimidazolium bromide (**21e**)

General procedure 2 was employed for the preparation of **21e**. Yield: 70%; R_f 0.46 ($\text{CHCl}_3/\text{MeOH}$ 9:1); t_R 15.31 min (70% MeCN → 100% MeCN in 30 min); ESI-MS (m/z): 1234.37 [M – Br] $^+$; ^1H NMR (400 MHz, CDCl_3) δ 7.92–7.85 (m, 2H), 7.43–7.40 (m, 5H), 7.33–7.06 (m, 27H), 6.89–6.80 (m, 12H), 5.69 (s, 2H), 5.61 (s, 2H), 4.48 (s, 2H), 2.54 (t, 2H, $J = 7.5$ Hz), 1.25–1.19 (m, 4H), 0.86 (t, 3H, $J = 7.5$ Hz).

4.14.3. 5-Butyl-4-chloro-2-hydroxymethyl-*N,N'*-bis[2'-(tert-butoxycarbonyl)biphenyl-4-yl]methylimidazolium bromide (**22c**)

The same procedure as above was employed for the preparation of **22c**. Yield: 78%; R_f 0.32 ($\text{CHCl}_3/\text{MeOH}$ 9:1); t_R 10.59 min (60% MeCN → 100% MeCN in 30 min); ESI-MS (m/z): 721.45 [M – Br] (^{35}Cl), 723.46 [M + 2 – Br] (^{37}Cl); ^1H NMR (400 MHz, CDCl_3): δ 7.78 (d, 2H, $J = 7.6$ Hz), 7.48 (t, 2H, $J = 7.5$ Hz), 7.40 (t, 2H, $J = 7.5$ Hz), 7.35–7.22 (m, 8H), 7.11 (d, 2H, $J = 7.6$ Hz), 5.86 (s, 2H), 5.79 (s, 2H), 4.83 (s, 2H), 2.68 (t, 2H, $J = 7.5$ Hz), 1.41–1.26 (m, 4H), 1.25 (s, 9H), 1.23 (s, 9H), 0.90 (t, 3H, $J = 7.5$ Hz).

4.14.4. 4-Bromo-5-butyl-2-hydroxymethyl-*N,N'*-bis[2'-(tert-butoxycarbonyl)biphenyl-4-yl]methylimidazolium bromide (**22d**)

The same procedure as above was employed for the preparation of **22d**. Yield: 75%; R_f 0.33 ($\text{CHCl}_3/\text{MeOH}$ 9:1); t_R 10.42 min (60% MeCN → 100% MeCN in 30 min); ESI-MS (m/z): 765.56 [M – Br] (^{79}Br), 767.57 [M + 2 – Br] (^{81}Br); ^1H NMR (400 MHz, CDCl_3): δ 7.79 (d, 2H, $J = 7.4$ Hz), 7.49 (t, 2H, $J = 7.3$ Hz), 7.41 (t, 2H, $J = 7.3$ Hz), 7.35–7.23 (m, 8H), 7.12 (d, 2H, $J = 7.6$ Hz), 5.92 (s, 2H), 5.84 (s, 2H), 4.82 (s, 2H), 2.70 (t, 2H, $J = 7.5$ Hz), 1.58–1.36 (m, 4H), 1.27 (s, 9H), 1.25 (s, 9H), 0.93 (t, 3H, $J = 7.1$ Hz).

4.14.5. 5-Butyl-2-hydroxymethyl-4-iodo-*N,N'*-bis[2'-(tert-butoxycarbonyl)biphenyl-4-yl]methylimidazolium bromide (**22e**)

The same procedure as above was employed for the preparation of **22e**. Yield: 74%; R_f 0.35 ($\text{CHCl}_3/\text{MeOH}$ 9:1); t_R 10.42 min (60% MeCN → 100% MeCN in 30 min); ESI-MS (m/z): 813.48 [M – Br]; ^1H NMR (400 MHz, CDCl_3): δ 7.79 (d, 2H, $J = 7.6$ Hz), 7.49 (t, 2H, $J = 7.4$ Hz), 7.41 (t, 2H, $J = 7.4$ Hz), 7.35–7.19 (m, 8H), 7.10 (d, 2H, $J = 7.6$ Hz), 5.90 (s, 2H), 5.83 (s, 2H), 4.79 (s, 2H), 2.73 (t, 2H, $J = 7.5$ Hz), 1.52–1.35 (m, 4H), 1.27 (s, 9H), 1.26 (s, 9H), 0.94 (t, 3H, $J = 7.5$ Hz).

4.15. 5-Butyl-4-chloro-2-hydroxymethyl-*N,N'*-bis[2'-[2H-tetrazol-5-yl]biphenyl-4-yl]methylimidazolium bromide (**23c**)

General procedure 3 was employed for the preparation of **23c**. Yield: 77%; R_f 0.35 ($\text{CHCl}_3/\text{MeOH}/\text{gl. AcOH}$ 9:1:0.1); t_R 12.78 min (20% MeCN → 100% MeCN in 30 min); ESI-MS (m/z): 657.20 [M – Br] (^{35}Cl), 659.23 [M + 2 – Br] (^{37}Cl); ^1H NMR (400 MHz, CD_3OD): δ 7.68–7.66 (m, 4H), 7.60–7.56 (m, 4H), 7.24–7.07 (m, 8H), 5.64 (s, 2H), 5.62 (s, 2H), 4.95 (s, 2H), 2.66 (t, 2H, $J = 7.5$ Hz), 1.36–1.29 (m, 4H), 0.83 (t, 3H, $J = 7.5$ Hz); ^{13}C NMR (160 MHz, CD_3OD): δ 155.32, 146.23, 143.96, 141.18, 140.06, 133.14, 132.62, 131.98, 131.12, 130.39, 130.17, 129.68, 129.53, 129.03, 127.89, 127.82, 126.96, 126.44, 125.86, 122.98, 54.39, 49.09, 29.14, 22.26, 21.68, 12.40.

4.15.1. 4-Bromo-5-butyl-2-hydroxymethyl-*N,N'*-bis[2'-[2H-tetrazol-5-yl]biphenyl-4-yl]methylimidazolium bromide (**23d**)

General procedure 3 was employed for the preparation of **23d**. Yield: 77%; R_f 0.34 ($\text{CHCl}_3/\text{MeOH}/\text{gl. AcOH}$ 9:1:0.1); t_R 12.78 min (20% MeCN → 100% MeCN in 30 min); ESI-MS (m/z): 701.40

[M – Br] (⁷⁹Br), 703.51 [M + 2 – Br] (⁸¹Br); ¹H NMR (400 MHz, CD₃OD): δ 7.65–7.63 (m, 4H), 7.55–7.51 (m, 4H), 7.18–7.03 (m, 8H), 5.60 (s, 2H), 5.59 (s, 2H), 4.90 (s, 2H), 2.61 (t, 2H, J = 7.5 Hz), 1.33–1.23 (m, 4H), 0.83 (t, 3H, J = 7.5 Hz); ¹³C NMR (160 MHz, CD₃OD): δ 156.74, 156.67, 146.69, 143.99, 141.12, 141.10, 140.53, 134.81, 133.58, 132.91, 132.45, 130.26, 129.76, 129.56, 127.77, 126.65, 126.27, 124.61, 107.35, 50.29, 49.22, 29.35, 23.06, 21.74, 12.46.

4.15.2. 5-Butyl-2-hydroxymethyl-4-iodo-N,N'-bis[[2'-(2H-tetrazol-5-yl)biphenyl-4-yl]methyl]imidazolium bromide (**23e**)

General procedure 3 was employed for the preparation of **23e**. Yield: 75%; *R*_f 0.36 (CHCl₃/MeOH/gl. AcOH 9:1:0.1); *t*_R 12.89 min (20% MeCN → 100% MeCN in 30 min); ESI-MS (*m/z*): 749.45 [M – Br]; ¹H NMR (400 MHz, CD₃OD): δ 7.65–7.58 (m, 4H), 7.49–7.42 (m, 4H), 7.14–7.09 (m, 8H), 5.59 (s, 4H), 4.91 (s, 2H), 2.61 (t, 2H, J = 7.5 Hz), 1.24–1.23 (m, 4H), 0.79 (t, 3H, J = 7.5 Hz); ¹³C NMR (160 MHz, CD₃OD): δ 158.32, 146.58, 141.49, 137.75, 134.59, 134.17, 131.53, 130.82, 130.25, 130.01, 129.51, 128.51, 127.77, 125.58, 89.58, 52.50, 51.54, 29.75, 22.48, 21.52, 12.55.

4.15.3. 5-Butyl-4-chloro-2-hydroxymethyl-N,N'-bis[[2'-carboxybiphenyl-4-yl]methyl]imidazolium bromide (**24c**)

General procedure 3 was employed for the preparation of **24c**. Yield: 81%; *R*_f 0.23 (CHCl₃/MeOH/gl. AcOH 8:2:0.2); *t*_R 16.99 min (10% MeCN → 100% MeCN in 30 min); ESI-MS (*m/z*): 609.39 [M – Br] (³⁵Cl), 611.34 [M + 2 – Br] (³⁷Cl); ¹H NMR (400 MHz, CD₃OD): δ 7.80 (d, 2H, J = 7.4 Hz), 7.49 (t, 2H, J = 7.4 Hz), 7.40–7.27 (m, 12H), 5.64 (s, 4H), 4.97 (s, 2H, H-6), 2.66 (t, 2H, J = 7.5 Hz), 1.30–1.23 (m, 4H), 0.78 (t, 3H, J = 7.5 Hz); ¹³C NMR (160 MHz, CD₃OD): δ 171.25, 147.78, 144.60, 142.62, 140.76, 134.59, 134.33, 134.08, 132.40, 132.32, 131.50, 131.38, 129.43, 128.82, 128.40, 121.96, 51.62, 51.48, 31.53, 24.68, 24.07, 14.70.

4.15.4. 4-Bromo-5-butyl-2-hydroxymethyl-N,N'-bis[[2'-carboxybiphenyl-4-yl]methyl]imidazolium bromide (**24d**)

General procedure 3 was employed for the preparation of **24d**. Yield: 77%; *R*_f 0.24 (CHCl₃/MeOH/gl. AcOH 8:2:0.2); *t*_R 16.91 min (10% MeCN → 100% MeCN in 30 min); ESI-MS (*m/z*): 653.34 [M – Br] (⁷⁹Br), 655.31 [M + 2 – Br] (⁸¹Br); ¹H NMR (400 MHz, CD₃OD): δ 7.78 (d, 2H, J = 7.3 Hz), 7.50 (t, 2H, J = 7.5 Hz), 7.41–7.23 (m, 12H), 5.65 (s, 4H), 4.98 (s, 2H), 2.66 (t, 2H, J = 7.3 Hz), 1.30–1.25 (m, 4H), 0.79 (t, 3H, J = 7.3 Hz); ¹³C NMR (160 MHz, CD₃OD): δ 172.13, 147.14, 142.65, 142.50, 140.94, 136.11, 135.26, 132.84, 132.39, 130.70, 130.64, 130.50, 129.59, 129.45, 127.55, 127.51, 126.81, 126.51, 107.77, 52.62, 50.79, 49.79, 29.78, 23.57, 22.23, 12.83.

4.15.5. 5-Butyl-2-hydroxymethyl-4-iodo-N,N'-bis[[2'-carboxybiphenyl-4-yl]methyl]imidazolium bromide (**24e**)

General procedure 3 was employed for the preparation of **24e**. Yield: 75%; *R*_f 0.25 (CHCl₃/MeOH/gl. AcOH 8:2:0.2); *t*_R 16.80 min (10% MeCN → 100% MeCN in 30 min); ESI-MS (*m/z*): 701.35 [M – Br]; ¹H NMR (400 MHz, CD₃OD): δ 7.78 (d, 2H, J = 7.4 Hz), 7.50 (td, 2H, J = 0.9, 7.4 Hz), 7.41–7.20 (m, 12H), 5.64 (s, 4H), 4.95 (br s, 2H), 2.67 (t, 2H, J = 7.4 Hz), 1.30–1.19 (m, 4H, H-8), 0.80 (t, 3H, J = 7.4 Hz); ¹³C NMR (160 MHz, CD₃OD): δ 171.53, 150.39, 144.49, 144.30, 142.76, 141.80, 134.95, 134.55, 132.38, 131.48, 131.33, 130.12, 129.43, 128.58, 128.37, 120.49, 120.16, 82.07, 54.73, 51.70, 32.12, 26.94, 24.23, 14.78.

4.16. 2-Butyl-N,N'-bis[[2'-[2-(trityl)tetrazol-5-yl]biphenyl-4-yl]methyl]imidazolium bromide (**25**)

General procedure 1 was employed for the preparation of **25**. Yield: 85%; m.p. 152–154 °C; *R*_f 0.50 (CHCl₃/MeOH, 96:4); *t*_R 15.61 min (70% MeCN → 100% MeCN in 30 min); ESI-MS (*m/z*):

1078.89 [M – Br], 835.61 [(M – Tr) + H – Br], 243.20 [Tr]; ¹H NMR (400 MHz, CDCl₃): δ 7.96–7.94 (m, 2H), 7.50–7.47 (m, 6H), 7.34–7.07 (m, 28H), 6.93–6.91 (m, 12H), 5.31 (s, 4H), 2.86 (t, 2H, J = 7.3 Hz), 1.30–1.22 (m, 4H), 0.79 (t, 3H, J = 7.3 Hz).

4.16.1. 2-Butyl-N,N'-bis[[2'-(tert-butoxycarbonyl)]biphenyl-4-yl]methylimidazolium bromide (**26**)

General procedure 1 was employed for the preparation of **26**. Yield: 84%; m.p. 148–151 °C; *R*_f 0.51 (CHCl₃/MeOH, 9:1); *t*_R 9.84 min (60% MeCN → 100% MeCN in 30 min); ESI-MS (*m/z*): 657.63 [M – Br]; ¹H NMR (400 MHz, CDCl₃): δ 7.80 (dd, 2H, J = 1.2, 7.6 Hz), 7.52 (s, 2H), 7.48 (dd, 2H, J = 1.2, 7.6 Hz), 7.42–7.36 (m, 10H), 7.27–7.25 (m, 2H), 5.58 (s, 4H), 3.26 (t, 2H, J = 7.2 Hz), 1.42–1.23 (m, 22H), 0.88 (t, 3H, J = 7.2 Hz).

4.17. 2-Butyl-N,N'-bis[[2'-(2H-tetrazol-5-yl)biphenyl-4-yl]methyl]imidazolium bromide (**27**)

General procedure 3 was employed for the preparation of **27**. Yield: 84%; *R*_f 0.30 (CHCl₃/MeOH/gl. AcOH, 9:1:0.1); *t*_R 11.66 min (20% MeCN → 100% MeCN in 30 min); ESI-MS (*m/z*): 593.39 [M – Br]; ¹H NMR (400 MHz, CD₃OD): δ 7.67–7.54 (m, 10H), 7.26–7.19 (m, 8H), 5.43 (s, 4H), 3.03 (t, 2H, J = 7.2 Hz), 1.36–1.28 (m, 4H), 0.84 (t, 3H, J = 7.2 Hz); ¹³C NMR (160 MHz, CD₃OD): δ 161.99, 147.76, 143.85, 140.88, 134.24, 132.98, 130.49, 130.27, 130.21, 129.77, 129.40, 127.74, 127.43, 124.22, 122.01, 51.07, 30.70, 21.98, 20.31, 12.35.

4.17.1. 2-Butyl-N,N'-bis[[2'-carboxybiphenyl-4-yl]methyl]imidazolium bromide (**28**)

General procedure 3 was employed for the preparation of **28**. Yield: 80%; m.p. 129–132 °C; *R*_f 0.22 (CHCl₃/MeOH/gl. AcOH, 8:2:0.2); *t*_R 16.13 min (10% MeCN → 100% MeCN in 30 min); ESI-MS (*m/z*): 545.46 [M – Br]; ¹H NMR (400 MHz, CD₃OD): δ 7.87 (d, 2H, J = 7.5 Hz), 7.65 (s, 2H), 7.59 (t, 2H, J = 7.5 Hz), 7.47–7.45 (m, 12H), 5.51 (s, 4H), 3.13 (t, 2H, J = 7.4 Hz), 1.39–1.30 (m, 4H), 0.87 (t, 3H, J = 7.4 Hz); ¹³C NMR (160 MHz, CD₃OD): δ 170.29, 147.84, 142.40, 141.35, 132.70, 131.29, 131.05, 131.40, 129.58, 129.18, 127.29, 122.03, 51.25, 28.23, 23.00, 22.07, 12.34.

4.18. 2-Butyl-4-chloro-5-hydroxymethyl-N,N'-bis[[2'-(2H-tetrazol-5-yl)biphenyl-4-yl]methyl]imidazolium bromide (**30**)

General procedures 6 and 3 were employed for the preparation of **30**. Yield: 77%; m.p. 159–162 °C; *R*_f 0.34 (CHCl₃/MeOH/gl. AcOH, 9:1:0.1); *t*_R 10.93 min (20% MeCN → 100% MeCN in 30 min); ESI-MS (*m/z*): 657.44 [M – Br] (³⁵Cl), 659.46 [M + 2 – Br] (³⁷Cl); ¹H NMR (400 MHz, CD₃OD): δ 7.68–7.64 (m, 4H), 7.59–7.30 (m, 5H), 7.27–7.20 (m, 7H), 5.66 (s, 2H), 5.58 (s, 2H), 4.65 (s, 2H), 2.71 (t, 2H, J = 7.5 Hz), 1.32–1.24 (m, 2H), 0.73 (t, 3H, J = 7.5 Hz).

4.19. 2-Butyl-4-chloro-5-hydroxymethyl-N,N'-bis[[2'-carboxybiphenyl-4-yl]methyl]imidazolium bromide (**31**)

General procedures 7 and 3 were employed for the preparation of **31**. Yield: 74%; m.p. 128–131 °C; *R*_f 0.20 (CHCl₃/MeOH/gl. AcOH, 8:2:0.2); *t*_R 16.11 min (10% MeCN → 100% MeCN in 30 min); ESI-MS (*m/z*): 609.26 [M – Br] (³⁵Cl), 611.21 [M + 2 – Br] (³⁷Cl); ¹H NMR (400 MHz, CD₃OD): δ 7.73 (d, 2H, J = 7.5 Hz), 7.46 (t, 2H, J = 7.5 Hz), 7.38–7.36 (m, 6H), 7.27–7.25 (m, 4H), 7.20 (d, 2H, J = 8.0 Hz), 5.62 (s, 2H), 5.54 (s, 2H), 4.63 (s, 2H), 3.01 (t, 2H, J = 7.2 Hz), 1.21 (quint, 2H, J = 7.2 Hz), 1.10 (sext, 2H, J = 7.2 Hz), 0.70 (t, 3H, J = 7.2 Hz); ¹³C NMR (160 MHz, CD₃OD): δ 174.11, 151.61, 144.60, 142.78, 135.77, 134.76, 134.30, 132.56, 132.39, 131.50, 131.31, 129.47, 128.56, 128.30, 122.46, 53.73, 51.76, 51.07, 30.59, 26.33, 24.30, 14.52.

4.20. Docking studies

The 3D model of the AT1 receptor used in our docking studies was kindly provided by Tuccinardi et al. [45]. The construction of this model is based on X-ray bovine rhodopsin structure, molecular procedure and available site-directed mutagenesis data [46]. Molecular Docking studies were performed using Glide extra precision (XP) implemented Induced Fit Docking (IFD) protocol (v5.0) [47–49] docking programs under the Linux operating system.

The binding site was defined by 20 Å inner cubic grid box, centered on the point that is the center of mass of residues Lys199 and His256. The IFD protocol under the Schrodinger molecular modeling package was used in order to eliminate clashes between receptor and ligand atoms and for the receptor to gain partial flexibility to the receptor. Before the docking simulations, the complexes were submitted to the protein preparation module of Schrodinger. Ligands were constructed using the Schrodinger's Maestro module and then geometry optimization was performed for these ligands using Polak–Ribiere conjugate gradient (PRCG) minimization ($0.0001 \text{ kJÅ}^{-1} \text{ mol}^{-1}$ convergence criteria). Protonation states of residues were created using LigPrep and Protein Preparation modules under the Schrodinger package at neutral pH. IFD uses the Glide docking program to account the ligand flexibility and the refinement module and the Prime (v.1.6) program [48,49] to account for flexibility of the receptor. Schrodinger's IFD protocol model uses the following steps (the description below is taken from the IFD user manual): (i) Constrained minimization of the receptor with an RMSD cutoff of 0.18 Å. (ii) Initial Glide docking of each ligand using soft potentials (0.5 van der Waals radii scaling of non-polar atoms of ligands and receptor using partial charge cutoff of 0.15). (iii) Derived docking poses were refined using the Prime Induced Fit module of Schrodinger. Residues within 5.0 Å of ligand poses were minimized in order to form suitable conformations of poses at the binding site of the receptor. (iv) Glide re-docking of each protein–ligand complex.

4.21. Molecular dynamics simulations

A lipid bilayer of 72 DPPC molecules was simulated under the CHARMM 36 force field [50,51] with all hydrogen atoms explicit, whereas the aqueous phase (2162 water molecules) was described by the TIP3P [52] (transferable intermolecular potential 3P) model. The initial structure for the bilayer was downloaded as a PDB file by the following web page: <http://terpconnect.umd.edu/~jbklauda/research/download.html>. As far as the **12b** molecule, its topology file was created by the SwissParam server which is available online: <http://swissparam.ch/> [53]. The abovementioned topology files are compatible with the CHARMM force field.

All simulations were performed with the molecular dynamics package GROMACS 4.5.4 [54–57] in the context of NP₂AT ensemble with a constant area per lipid, *A*, equal to $0.64 \text{ nm}^2/\text{lipid}$. The equations of motion were integrated with a time step equal to 2 fs while temperature was kept constant at 317 K using the Berendsen thermostat [58] with a coupling time constant equal to 0.1 ps. Regarding to the pressure along the normal to two DPPC leaflets (*Z*-axis), it was regulated by the Berendsen barostat [58] at 1 bar, with a coupling time constant to be 1 ps. Lennard–Jones and Coulomb interactions were calculated using a 1.0 nm cut-off radius while the long range electrostatics were treated with the Particle Mesh Ewald (PME) method [59]. The system was energy-minimized employing the steepest descent method [57] and after that the MD simulation was commenced with the **12b** molecule initially placed in the aqueous phase. The whole duration of the simulation is equal to 120 ns whereas the last 40 ns were employed for the calculation of the properties.

4.22. Umbrella sampling simulations

The PMF of the **12b** from aqueous to lipid phase was computed by the Weighted Histogram Analysis Method (WHAM) [60,61] that is available in GROMACS 4.5.4. In particular, thirty one biasing MD simulations were conducted along a reaction coordinate ζ (*Z*-axis), which is defined as the distance of the **12b** center of mass from the bilayer center ($\zeta = 0$). In addition, a harmonic potential was applied ($k = 500 \text{ kJ/mol/nm}^2$) between bilayer and **12b** centers of mass. It has also to be reported that the simulation system contains 3021 water molecules so as to avoid the interaction of the drug with the periodic image of the opposite leaflet of the bilayer. The duration of the biasing MD simulations was 24 ns of which the first 10 ns was regarded as an equilibration and therefore they were not taken into account for the computation of PMF. The rest of the MD parameters were the same with those given in the previous subsection.

4.23. Quantum chemical calculations

Geometry optimization and HOMO and LUMO calculations were performed for the studied compounds. The geometries were fully optimized using Density Functional Theory (DFT) hybrid method with the Becke's three-parameter exchange functional and gradient-corrected functional of Lee, Yang and Parr (B3LYP) [62] using the following standard basis set: 3–21 g. All geometry optimization were followed by calculations of frequencies in order to identify obtained structures as energy minima (no imaginary frequencies). All minima for all the compounds were verified by establishing that the matrix of energy second derivatives (Hessian) has only positive eigenvalues (all vibrational frequencies are real). All calculations were carried out with the Gaussian 09W program.

HOMO and LUMO frontier orbitals of the molecule were also computed at the same level of theory. Molecular orbital (MO) surfaces visually represent the various stable electron distributions of a molecule. According to Frontier orbital theory [63] the shapes and symmetries of the highest-occupied and lowest-unoccupied molecular orbitals (HOMO and LUMO) are crucial in predicting the reactivity of a species and the stereochemical and regiochemical outcome of a chemical reaction. Molecules with high HOMO (highest occupied molecular orbital energy) values are able to donate electron density more easily than molecules with low HOMO energy values. The HOMO energy value can be increased with the presence of electron-donating groups (EDG) such as $-\text{NMe}_2$, $-\text{NH}_2$, $-\text{NHEt}$, and $-\text{OMe}$ and decreased with the presence of electron-withdrawing groups (EWG) such as halogens, $-\text{CN}$ and $-\text{NO}_2$ groups [64].

4.24. Pharmacological evaluation

4.24.1. AT1 receptor binding assay of synthesized ANGII analogs

4.24.1.1. Cell culture and transfection. Human embryonic kidney (HEK 293) cells were grown in DMEM/F12 (1:1) containing 3.15 g/L glucose and 10% bovine calf serum at 37 °C and 5% CO₂. 60 mm dishes of HEK 293 cells at 80–90% confluence were transfected with 3 μg of plasmid DNA encoding the human AT1 receptor, using 9 μL of Lipofectamine and 2 mL of OPTIMEM. To generate stably transfected pools of cells expressing the AT1 receptor 5–12 h after transfection, the medium was replaced by DMEM/F12 (1:1) containing 3.15 g/L glucose, 10% bovine calf serum and 700 μg/mL of the antibiotic, Geneticin. The antibiotic used ensured the selection of a stably transfected pool of cells.

4.24.1.2. Harvesting cells and membrane preparation. HEK 293 cells (grown in 100 mm dishes) stably expressing the human AT1 receptor were washed with phosphate-buffered saline (PBS; 4.3 mM

Na₂HPO₄·7H₂O, 1.4 mM KH₂PO₄, 137 mM NaCl, 2.7 mM KCl, pH 7.2–7.3 at room temperature), briefly treated with PBS containing 2 mM EDTA (PBS/EDTA), and then dissociated in PBS/EDTA. Cell suspension was centrifuged at 1000× g for 5 min at room temperature, and the pellet was homogenized in 1 mL of buffer O (50 mM Tris–HCl containing 0.5 mM EDTA, 10% sucrose, 10 mM MgCl₂, pH 7.4 at 4 °C) using a Janke & Kunkel IKA Ultra Turrax T25 homogenizer (at setting ~20, 10–15 s, 4 °C). The homogenate was centrifuged at 250× g for 5 min at room temperature. The pellet was discarded and the supernatant was centrifuged (16,000× g, 10 min, 4 °C). The membrane pellet was resuspended (0.6–0.7 mL/100 mm dish) in buffer B (50 mM Tris–HCl containing 1 mM EDTA, 10 mM MgCl₂, 0.2% BSA, 0.2 mg/mL bacitracin, and 0.93 µg/mL aprotinin, pH 7.4 at 4 °C) and used for radioligand binding studies.

4.24.1.3. [¹²⁵I-Sar¹-Ile⁸] ANGII binding. The [¹²⁵I-Sar¹-Ile⁸] ANGII competition binding was performed as follows. Aliquots of diluted membrane suspension (50 µL) were added into tubes, containing buffer B and 100,000–120,000 cpm [¹²⁵I-Sar¹-Ile⁸] ANGII with or without increasing concentrations of ANGII analogs in a final volume of 0.15 mL. The mixtures were incubated (1 h, 24 °C) and then, filtered using a Brandel cell harvester through Whatman GF/C glass fiber filters, presoaked for 1 h in 0.5% polyethyleneimine at 4 °C. The filters were washed 10 times with 1–2 mL of ice-cold 50 mM Tris–HCl containing NaCl 120 mM, pH 7.4 at 4 °C. Filters were assessed for radioactivity in a gamma counter (LKB Wallac 1275 minigamma, 80% efficiency). The amount of membrane used was adjusted to ensure that specific binding was always equal to or less than 10% of the total concentration of the radioligand added. Specific [¹²⁵I-Sar¹-Ile⁸] ANGII binding was defined as the total binding minus non-specific binding in the presence of 1000 nM [Sar¹-Ile⁸] ANGII. Data analysis for competition binding was performed by nonlinear regression analysis, using GraphPad Prism 4.0 (GraphPad Software, San Diego, CA). –logIC₅₀ values were obtained by fitting the data from competition studies to a one-site competition model and presented as mean plus/minus standard error (SE).

4.24.2. Rat uterotonic test *in vitro*

The compounds prepared were tested in rat uterotonic *in vitro* test [65]. All samples were dissolved in DMSO to make stock solution of 1–4 mg/mL. Further solutions were made in physiological solution. Standard ANGII was dissolved in physiological solution. The test was performed in the same way as described for oxytocin and vasopressin analogs or bradykinin compounds [65–68]. The pA₂ was calculated from at least 3 independent experiments using uteri from different rats. In brief, the excised and longitudinally cut strips of rat uterus were placed into a bathing chamber into media without magnesium ions and mounted to the contraction recorder. The height of a single isometric contraction of a uterine strip was measured. The cumulative dose–response curves of standard ANGII were constructed, i.e. doses of standard (in the presence or absence of an analog) were added successively to the uterus in the organ bath in doubling concentrations and at 1 min intervals without the fluid being changed until the maximal response (the highest contraction) was obtained. The shift of the curves in the presence of an analog was determined. The concentration of the analog leading to the shift corresponding to 0.3 in logarithmic scale (it means that twice higher concentration of the standard was necessary to apply to reach the half maximal effect) was determined. Negative logarithm on the base of 10 of that concentration is pA₂. Wistar rats were used in all experiments. Handling of the experimental animals was done under supervision of the Ethics Committee of the Academy of Sciences according to § 23 of the law of the Czech Republic no. 246/1992.

Author contribution

Organic Synthesis: George Agelis, Amalia Resvani, John Matsoukas, **Structure Elucidation, Docking Studies, Molecular Dynamics & Biological Evaluation:** Catherine Koukoulitsa, Tereza Tůmová, Jiřina Slaninová, Dimitra Kalavrizioti, Katerina Spyridaki, Antreas Afantitis, Georgia Melagraki, Athanasia Siafaka, Eleni Gkini, Grigorios Megariotis, Simona Golic Grdadolnik, Manthos G. Papadopoulos, Demetrios Vlahakos, George Liapakis, Michael Maragoudakis, Thomas Mavromoustakos.

Acknowledgments

This project was supported by the pharmaceutical companies ELDRUG SA and VIANEX SA. We also acknowledge Demetrios Vahlitiotis (Instrumental Analysis Laboratory, University of Patras) for recording the NMR spectra. Prof. T. Mavromoustakos acknowledges EENC program for covering the travel and residence expenses to perform NMR experiments in the Slovenian. The NMR studies were supported by EN-FIST Center of Excellence (Dunajska 156, SI-1000 Ljubljana, Slovenia) and the Slovenian Research Agency. K.K. acknowledges Greek national funds through the Operational Program “Education and Lifelong Learning” of the National Strategic Reference Framework(NSRF)–Research Funding Program: Heracleitus II, investing in knowledge society through the European Social Fund.

Appendix A. Supplementary data

Supplementary data related to this article can be found at <http://dx.doi.org/10.1016/j.ejmech.2012.12.044>.

References

- [1] C. Dagupta, L. Zhang, *Drug Discov. Today* 16 (1–2) (2011) 22–34.
- [2] N. Prashant, P. Murmkar, R. Girdhar, M.R. Yadav, *Bioorg. Med. Chem.* 18 (2010) 8418–8456.
- [3] J.V. Duncia, A.T. Chiu, D.J. Carini, G.B. Gregory, A.L. Johnson, W.A. Price, G.J. Wells, P.C. Wong, J.C. Calabrese, *J. Med. Chem.* 33 (1990) 1312–1329.
- [4] K. Kubo, Y. Kohara, E. Imamiya, Y. Sigiura, Y. Inada, Y. Furukawa, K. Nishikawa, T. Naka, *J. Med. Chem.* 36 (1993) 2182–2195.
- [5] P. Buhlmayer, P. Furet, L. Criscione, M. de Gasparo, S. Whitebread, T. Schmidlin, R. Lattmann, J. Wood, *Bioorg. Med. Chem. Lett.* 4 (1994) 29–34.
- [6] C.A. Bernhart, P.M. Perreaut, B.P. Ferrari, Y.A. Muneaux, J.-L.A. Assenes, J. Clement, F. Haudricourt, C.F. Muneaux, J.E. Taillades, M.-A. Vignal, J. Gougat, P.R. Guiraudou, C.A. Lacour, A. Roccon, C.F. Cazaubon, J.-C. Breliere, G. Le Fur, D. Nisato, *J. Med. Chem.* 36 (1993) 3371–3380.
- [7] U.J. Ries, G. Mihm, B. Narr, K.M. Hasselbach, H. Wittenben, M. Entzeroth, J.C.A. Van Meel, W. Wiene, N.H. Haeuel, *J. Med. Chem.* 36 (1993) 4040–4051.
- [8] H. Yanagisawa, Y. Ameniya, T. Kanazaki, Y. Shimoji, K. Fujimoto, Y.M. Kitahara, T. Sada, M. Mizuno, M. Ikeda, S. Miyamoto, Y.M. Furukawa, H. Koike, *J. Med. Chem.* 39 (1996) 323–338.
- [9] Y. Kohara, K. Kubo, E. Imamiya, T. Wada, Y. Inada, T. Naka, *J. Med. Chem.* 39 (1996) 5228–5235.
- [10] W.L. Baker, W.B. White, *Ann. Pharmacother.* 45 (2011) 1506–1515.
- [11] V. Papademetriou, M. Dumas, K. Tsioufis, *Int. J. Hypertens.* (2011) 2–8.
- [12] D.J. Carini, J.V. Duncia, P.E. Aldrich, A.T. Chiu, A.L. Johnson, M.E. Pierce, W.A. Price, J.B. Santella, G.J. Wells, R.R. Wexler, P.C. Wong, S.E. Yoo, P.B.M.W.M. Timmermanns, *J. Med. Chem.* 34 (1991) 2525–2547.
- [13] N. Kaur, A. Kaur, Y. Bansal, D.V. Shah, G. Bansal, M. Singh, *Bioorg. Med. Chem.* 16 (2008) 10210–10215.
- [14] A. Cappelli, C. Nannicini, G. Giuliani, S. Valenti, G.P. Mohr, M. Anzini, L. Mennuni, F. Ferrari, G. Caselli, A. Giordani, W. Peris, F. Makovec, G. Giorgi, S. Vomero, *J. Med. Chem.* 51 (2008) 2137–2146.
- [15] A. Catalano, A. Carocci, A. Di Mola, C. Bruno, P.M.L. Vanderheyden, C. Franchini, *Arch. Pharm. Life Sci.* 344 (2011) 617–626.
- [16] A. Wahhab, J.R. Smith, R.C. Ganter, D.M. Moore, J. Hondrelis, J. Matsoukas, G.J. Moore, *Arzn.-Forsch./Drug Res.* 43 (1993) 1157–1168.
- [17] G. Agelis, P. Roumelioti, A. Resvani, S. Durdagi, M.-E. Androutsou, K. Kelaidonis, T. Mavromoustakos, J. Matsoukas, *J. Comput. Aided Mol. Des.* 24 (2010) 749–758.
- [18] G. Agelis, A. Resvani, M.T. Matsoukas, T. Tselios, K. Kelaidonis, D. Kalavrizioti, D. Vlahakos, J. Matsoukas, *Amino Acids* 40 (2011) 411–420.

- [19] G. Agelis, A. Resvani, S. Durdagi, K. Spyridaki, T. Tümová, J. Slaninová, P. Giannopoulos, D. Vlahakos, G. Liapakis, T. Mavromoustakos, J. Matsoukas, *Eur. J. Med. Chem.* 55 (2012) 358–374.
- [20] B. Iddon, B.L. Lim, *J. Chem. Soc. Perkin Trans. 1* (1983) 735–739.
- [21] K.L. Kirk, *J. Heterocycl. Chem.* 22 (1985) 57–59.
- [22] R.K. Griffith, R.A. DiPietro, *Synth. Commun.* 16 (14) (1986) 1761–1770.
- [23] A.R. Katritzky, G.M. Rewcastle, W.-Q. Fan, *J. Org. Chem.* 53 (1988) 5685–5689.
- [24] C. Subramanyam, 4-Methoxybenzyl (PMB), *Synth. Commun.* 25 (5) (1995) 761–774.
- [25] J.W. Kim, S.M. Abdelaal, L. Bauer, N.E. Heimer, *J. Heterocycl. Chem.* 32 (1995) 611–620.
- [26] S.J. Yoo, H.O. Kim, Y. Lim, J. Kim, L.S. Jeong, *Bioorg. Med. Chem.* 10 (2002) 215–226.
- [27] G. Agelis, N. Tzioumaki, T. Botić, A. Cencić, D. Komiotis, *Bioorg. Med. Chem.* 15 (2007) 5448–5456.
- [28] S. Harusava, Y. Murai, H. Moriyama, T. Imazu, H. Ohishi, R. Yoneda, T. Kurihara, *J. Org. Chem.* 61 (1996) 4405–4411.
- [29] M.E. Pierce, D.J. Carini, G.F. Huhn, G. Wells, J.F. Arnett, *J. Org. Chem.* 58 (1993) 4642–4646.
- [30] W.C. Guida, D.J. Mathre, *J. Org. Chem.* 45 (1980) 3172–3176.
- [31] M. Sonogawa, M. Yokota, H. Tomiyama, T. Tomiyama, *Chem. Pharm. Bull.* 54 (5) (2006) 706–710.
- [32] T. Mavromoustakos, A. Kolocouris, M. Zervou, P. Roumelioti, J. Matsoukas, R. Weisemann, *J. Med. Chem.* 42 (10) (1999) 1714–1722.
- [33] C. Potamitis, M. Zervou, V. Katsiaras, P. Zoumpoulakis, S. Durdagi, M. Papadopoulos, J. Hayes, S. Grdadolnik, I. Kyrikou, D. Argyropoulos, G. Vatougia, T. Mavromoustakos, *J. Chem. Inf. Mod.* 49 (2009) 726–739.
- [34] P. Zoumpoulakis, S.G. Grdadolnik, J. Matsoukas, T. Mavromoustakos, *J. Pharmaceut. Biomed. Anal.* 28 (2002) 125–135.
- [35] P. Zoumpoulakis, A. Politi, S.G. Grdadolnik, J. Matsoukas, T. Mavromoustakos, *J. Pharmaceut. Biomed. Anal.* 40 (5) (2006) 1097–1104.
- [36] P. Zoumpoulakis, I. Daliani, M. Zervou, I. Kyrikou, E. Siapi, G. Lamprinidis, E. Mikros, T. Mavromoustakos, *Chem. Phys. Lipids* 125 (2003) 13–25.
- [37] M. Lucio, J.L.F.C. Lima, S. Reis, *Curr. Med. Chem.* 17 (2010) 1795–1809.
- [38] A.M. Seddon, D. Casey, R.V. Law, A. Gee, R.H. Templer, *O. Ces. Chem. Soc. Rev.* 38 (2009) 2509–2519.
- [39] E.F. Petersen, T.D. Goddard, C.C. Huang, G.S. Couch, D.M. Greenblatt, E.C. Meng, T.E. Ferrin, *J. Comput. Chem.* 25 (2004) 1605–1612.
- [40] A. Afantitis, G. Melagraki, H. Sarimveis, P.A. Koutentis, O. Igglessi-Markopoulou, G.A. Kollias, *Mol. Divers.* 14 (2) (2010) 225–235.
- [41] D. Ntountaniotis, G. Mali, S. Golic Grdadolnik, M. Halabalaki, A.L. Skaltsounis, C. Potamitis, E. Siapi, P. Chatzigeorgiou, M. Rappolt, T. Mavromoustakos, *Biochim. Biophys. Acta* 1808 (2011) 2995–3006.
- [42] A. Hodzic, P. Zoumpoulakis, G. Pabst, T. Mavromoustakos, M. Rappolt, *Phys. Chem. Chem. Phys.* 14 (2012) 4780–4788.
- [43] C. Fotakis, D. Christodouleas, P. Zoumpoulakis, A. Gili, E. Kritsi, N.-P. Benetis, M. Zervou, H. Reis, M. Papadopoulos, T. Mavromoustakos, *J. Chem. Phys. B* 115 (2011) 6180–6192.
- [44] C. Potamitis, P. Chatzigeorgiou, E. Siapi, T. Mavromoustakos, A. Hodzic, F. Cacho-Nerin, P. Laggner, M. Rappolt, *Biochim. Biophys. Acta* 1808 (2011) 1753–1763.
- [45] T. Tuccinardi, V. Calderone, S. Rapposelli, A. Martinelli, *J. Med. Chem.* 49 (2006) 4305–4316.
- [46] T. Okada, M. Sugihara, A.N. Bondar, M. Elstner, P. Entel, V. Buss, *J. Mol. Biol.* 342 (2004) 571–583.
- [47] R.A. Friesner, R.B. Murphy, M.P. Repasky, L.L. Frye, J.R. Greenwood, T.A. Halgren, P.C. Sanschagrin, D.T. Mainz, *J. Med. Chem.* 49 (2006) 6177–6196.
- [48] W. Sherman, T. Day, M.P. Jacobson, R.A. Friesner, R. Farid, *J. Med. Chem.* 49 (2006) 534–553.
- [49] L.L.C. Schrodinger, Portland, OR, 2007, Web address www.schrodinger.com.
- [50] J.B. Klauda, R.M. Venable, J.A. Freites, J.W. O'Connor, D.J. Tobias, C. Mondragon-Ramirez, I. Vorobyon, A.D. MacKerell, R.W. Pastor, *J. Phys. Chem.* 114 (2010) 7830–7843.
- [51] R.W. Pastor, A.D. MacKerell, *J. Phys. Chem. Lett.* 2 (2011) 1526–1532.
- [52] W.L. Jorgensen, J. Chandrasekhar, J.D. Madura, R.W. Impey, M.L. Klein, *J. Chem. Phys.* 79 (1983) 926–935.
- [53] V. Zoete, M.A. Cuendet, A. Grosdidier, O. Michielin, *J. Comput. Chem.* 32 (2011) 2359–2368.
- [54] H.J.C. Berendsen, D. van der Spoel, R. van Drunen, *Comp. Phys. Commun.* 91 (1995) 43–56.
- [55] D. Van der Spoel, E. Lindahl, B. Hess, G. Groenhof, A.E. Mark, H.J.C. Berendsen, *J. Comp. Chem.* 26 (2005) 1701–1718.
- [56] B. Hess, C. Kutzner, D. van der Spoel, E. Lindhal, *J. Chem. Theory Comp.* 4 (2008) 435–447.
- [57] D. van der Spoel, E. Lindahl, B. Hess, A.R. van Buuren, E. Apol, P.J. Meulenhoff, A. Sijbers, K.A. Feenstra, R. van Drunen, H.J.C. Berendsen, GROMACS User Manual, Version 4.5 (2010). Nijenborgh 4, www.gromacs.org.
- [58] H.J.C. Berendsen, J.P.M. Postma, A. DiNola, J.R. Haak, *J. Chem. Phys.* 81 (1984) 3684–3690.
- [59] U. Essmann, L. Perera, M.L. Berkowitz, T. Darden, H. Lee, L.G. Pedersen, *J. Chem. Phys.* 103 (1995) 8577–8593.
- [60] S. Kumar, J.M. Rosenberg, D. Bouzida, R.H. Swendsen, P.A. Kollman, *J. Comput. Chem.* 13 (1992) 1011–1021.
- [61] J.S. Hub, B.L. de Groot, D. van der Spoel, *J. Chem. Theory Comput.* 6 (2010) 3713–3720.
- [62] H.-Y. Wang, P.-S. Zhao, R.-Q. Li, S.-M. Zhou, *Molecules* 14 (2009) 608–620.
- [63] V. Stefanou, D. Matiadis, G. Melagraki, A. Afantitis, G. Athanasellis, O. Igglessi-Markopoulou, V. McKee, J. Markopoulos, *Molecules* 16 (2011) 384–402.
- [64] R. Todeschini, V. Consonni, R. Mannhold, in: H. Kubinyi, H. Timmerman (Eds.), *Handbook of Molecular Descriptors*, Wiley-VCH, Weinheim, 2000, pp. 362–363.
- [65] J. Slaninová, *Fundamental biological evaluation*, in: K. Jošt, M. Lebl, F. Brtník (Eds.), *Handbook of Neurohypophyseal Hormone Analogs*, vol. I, CRC Press Inc., Boca Raton, FL, 1987, pp. 83–107. Part 2.
- [66] V. Magafa, L. Borovicková, J. Slaninová, P. Cordopatis, *Amino Acids* 38 (2010) 1549–1559.
- [67] D. Sobolewski, A. Prahl, A. Kwiatkowska, J. Slaninová, B. Lammek, *J. Pept. Sci.* 15 (2009) 161–165.
- [68] O. Labudda, T. Wierzba, D. Sobolewski, W. Kowalczyk, M. Sleszyńska, L. Gawiński, M. Plackova, J. Slaninová, A. Prahl, *J. Pept. Sci.* 12 (2006) 775–779.